POLITECNICO DI TORINO
I Faculty of Engineering
Department of Mechanical and Aerospace Engineering

Master of Science in Automotive Engineering

Master Thesis

Development of a model for the estimation of exhaust gas recirculation in a spark ignition engine

Advisors at CRF:

Ing. Ceres Pasquale

Ing. Filippo Menzio

Advisors at Polito:

Prof. Ezio Spessa

Ing. Stefano d'Ambrosio

Ing. Daniela Misul

Daniel Ascione Martinez

October 2013

INTRODUCTION

Due to environmental pollution, the automotive industry is forced to meet with lowered emission demands legislated by the government. Improved technologies for engines control are essential. In recent years, the use of Exhaust Gas Recirculation (EGR) in Diesel engines has contributed to reducing emissions and achieve the limit.

Currently being developed gasoline engines that work with the EGR system, which not only reduce the environmental impact if not simultaneously decreases the fuel consumption.

The aim of this thesis is to propose a new computational model for the control valve that regulates the exhaust gas recirculation passage through the low pressure loop (LPL). Data provided by test bench is crucial for the model verification phase in order to compare the real data against the data obtained through the software.

The measurements in this thesis will be performed on a four cylinder gasoline engine with a long EGR route implementation. The model will be developed and tested using the Model Development Strategies (MDS), software developed in Centro Ricerche Fiat (CRF), simulation will be performed as follow: the first phase consisted in take a sample of the whole data base to perform the program, and the second phase is compare the model against the other methods already present in the module to realise the same work and then select the solution more precise.

Data were collected at different engine speeds, 2500, 3000 and 4000 rpm and using the equation for compressible flow nozzle is possible to describe the behavior of the EGR throttle valve with high precision.

ACKNOWLEDGMENTS

My deepest gratitude goes first and foremost to Prof. d'Ambrosio, for his constant encouragement and guidance. It is not only with great sense of responsibility serious academic attitude, but also he is a friendly professor. I extend my thanks to Filippo Menzio and Ceres Pasquale they were my tutors at Centro Ricerche Fiat, but also has they given me assistances and advices during the developing of the thesis.

Last but not least, the acknowledgement to my family, the give me full support without any complain or hesitation.

CONTENTS

LIST OF FIGURES

LIST OF TABLES

Part I

THEORETICAL BASIS

During the thesis a computational model to manage the EGR throttle valve is developed in order to control the quantity of EGR mass flow in the low pressure system.

The implementation of EGR gases allow the control of the pollutant emissions and the reduction of the fuel consumption (reducing the pumping losses) in a gasoline engine; therefore, general aspects of these type of engines will be described, developing in details the formation mechanism and description of pollutants that are emitted, which are the different configurations to implement the EGR solution, the benefits and drawbacks of the EGR in gasoline engines and description of the theory related to the throttle valve.

1

SPARK IGNITION ENGINES

1.1 GENERAL ASPECTS

In conventional SI engines the air and fuel are usually mixed together in the intake system prior to entry to the engine cylinder, using a carburetor or fuel-injection system. In automobile applications, the temperature of the air entering the intake system is controlled by mixing ambient air with air heated by contact with the exhaust manifold. The ratio of mass flow of air to mass flow of fuel must be held approximately constant at about 15 to ensure reliable combustion. The carburetor meters an appropriate fuel flow for the engine air flow in the following manner. The air flow through the venturi duct (a converging-diverging nozzle) sets up a pressure difference between the venturi inlet and throat which is used to meter an appropriate amount of fuel from the float chamber, through a series of orifices into the air flow at the venturi throat. Just downstream of the venturi is a throttle valve or plate which controls the combined air and fuel flow, and thus the engine output. The intake flow is throttled to below atmospheric pressure by reducing the flow area when the power required (at any engine speed) is below the maximum which is obtained when the throttle is wide open. The intake manifold is usually heated to promote faster evaporation of the liquid fuel and obtain more uniform fuel distribution between cylinders. [1]

Fuel injection into the intake manifold or inlet port is an increasingly common alternative to a carburetor. With port injection, fuel is injected through individual injectors from a low-pressure fuel supply system into each intake port. There are several different types of systems: mechanical injection using an injection pump driven by the engine; mechanical, driveless, continuous injection; electronically controlled, driveless, injection.

The sequence of events which take place inside the engine cylinder is illustrated in Figure (1). Crank angle is a useful independent

variable because engine processes occupy almost constant crank angle intervals over a wide range of engine speeds. The Fig. (1) shows the valve timing and volume relationship for a typical automotive spark-ignition engine. To maintain high mixture flows at high engine speeds (and hence high power outputs) the inlet valve, which opens before TC, closes substantially after BC. During intake, the inducted fuel and air mix in the cylinder with the residual burned gases remaining from the previous cycle. After the intake valve closes, the cylinder contents are compressed to above atmospheric pressure and temperature as the cylinder volume is reduced. Some heat transfer to the piston, cylinder head, and cylinder walls occurs but the effect on unburned gas properties is modest.

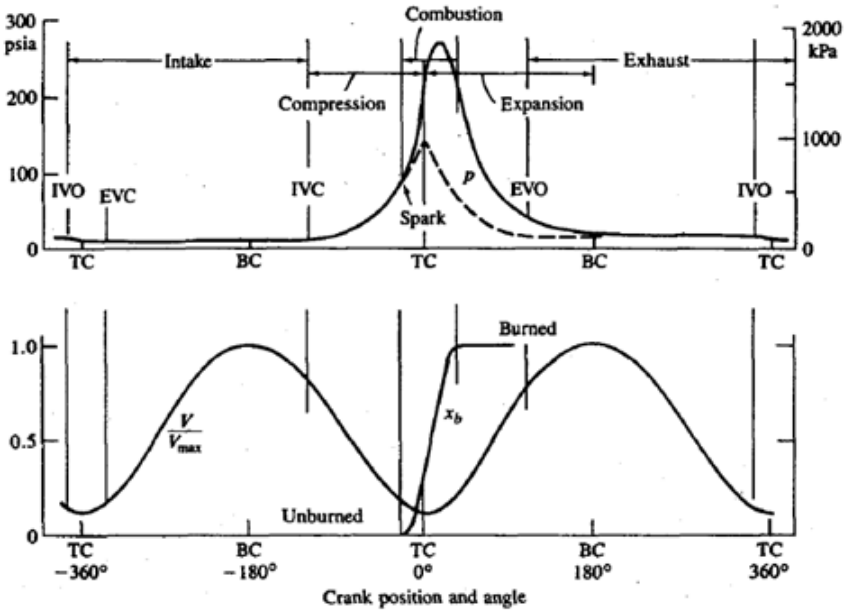

Figure 1: Sequence of events in four-stroke engine operating cycle. Cylinder pressure p (solid line, firing cycle; dashed line, motored cycle), cylinder volume V/V_{max}, and mass fraction burned x_b are plotted against crank angle

Between 10 and 40 crank angle degrees before TC an electrical discharge across the spark plug starts the combustion process. A distributor, a rotating switch driven off the camshaft, interrupts the current from the battery through the primary circuit of the ignition coil. The secondary winding of the ignition coil, connected to the spark plug, produces a high voltage across the plug electrodes as the magnetic field collapses. Traditionally, cam-operated breaker points have been used; in most automotive engines, the switching is now done electronically.

A turbulent flame develops from the spark discharge, propagates across the mixture of air, fuel, and residual gas in the cylinder, and extinguishes at the combustion chamber wall. The duration of this burning process varies with engine design and operation, but is typically 40 to 60 crank angle degrees, as shown in Figure (1). As fuel-air mixture burns in the flame, the cylinder pressure in Figure (1) (solid line) rises above the level due to compression alone (dashed line). This latter curve-called the motored cylinder pressure is the pressure trace obtained from a motored or non firing engine. Note that due to differences in the flow pattern and mixture composition between cylinders, and within each cylinder cycle-by-cycle, the development of each combustion process differs somewhat.

As a result, the shape of the pressure versus crank angle curve in each cylinder, and cycle-by-cycle, is not exactly the same. There is an optimum spark timing which, for a given mass of fuel and air inside the cylinder, gives maximum torque. More advanced (earlier) timing or retarded (later) timing than this optimum gives lower output. Called maximum brake - torque (MBT) timing, this optimum timing is an empirical compromise between starting combustion too early in the compression stroke (when the work transfer is to the cylinder gases) and completing combustion too late in the stroke (and so lowering peak expansion stroke pressures).

About two-thirds of the way through the expansion stroke, the exhaust valve starts to open. The cylinder pressure is greater than the exhaust manifold pressure and a blow down process occurs. The burned gases flow through the valve into the exhaust port and manifold until the cylinder pressure and exhaust pressure achieve the equilibrium. The duration of this process depends on the pressure level in the cylinder. The piston then displaces the burned gases from the cylinder into the manifold during the exhaust stroke. The exhaust valve opens before the end of the expansion stroke to ensure that the blow down process does not last too far into the exhaust stroke. The actual timing is a compromise which balances reduced work transfer to the piston before BC against reduced work transfer to the cylinder contents after BC.

The exhaust valve remains open until just after TC; the intake opens just before TC. The valves are opened and closed slowly to avoid noise and excessive cam wear. To ensure the valves are fully open when piston velocities are at their highest, the valve open periods often overlap. If the intake flow is throttled to below

exhaust manifold pressure, then back flow of burned gases into the intake manifold occurs when the intake valve is first opened.

1.2 POLLUTANTS EMISSIONS AND FORMATION MECHANISMS

Spark-ignition and diesel engines are a major source of urban air pollution. The spark-ignition engine exhaust gases contain oxides of nitrogen (nitric oxide, NO, and small amounts of nitrogen dioxide, NO_2, carbon monoxide (CO), and organic compounds which are unburned or partially burned hydrocarbons (HC).

The details of the basic formation mechanisms of each pollutant and the application of these mechanisms to the combustion process in a spark-ignition engine will be developed.

1.2.1 *Carbon monoxide CO*

CO formation occurs during the oxidation process of hydrocarbons, which is performed through the following steps:

$$RH \rightarrow R \rightarrow RO_2(peroxides) \rightarrow RCHO(aldehydes) \rightarrow RCO(ketones) \rightarrow CO$$

Where "R" is the generic radical. Finally, CO is oxidized to CO_2. However, the oxidation reaction of CO to CO_2 is quite slow if compared with the previous reaction steps above shown: therefore in rich mixtures all the fuel may start the oxidation process and reach the intermediate oxidation level of CO, but only part of the CO formed will be able to reach the complete oxidation level corresponding to CO_2 (about 3% volume should be expected at $\lambda = 0.9$).

CO oxidation to CO_2, if a suitable amount of oxygen is available, takes place according to the following reaction:

$$CO + OH \rightarrow CO_2 + H$$

At the high temperatures which are reached during the combustion process ($T \approx 2800^{\circ}K$), reaction rates are high enough to

reach a chemical equilibrium. Thank to the reverse reaction that leads to the dissociation of CO_2 into CO and OH, significant CO concentrations are to be expected; even if a sufficient amount of oxygen is present to fully oxidize CO to CO_2.

During the expansion period the sudden temperatures decrease, "freezes" the chemical reactions preventing further CO oxidation to CO_2. Therefore CO concentrations which are found in the exhaust are significantly higher than those that could be expected on the basis of chemical equilibrium at exhaust temperatures.

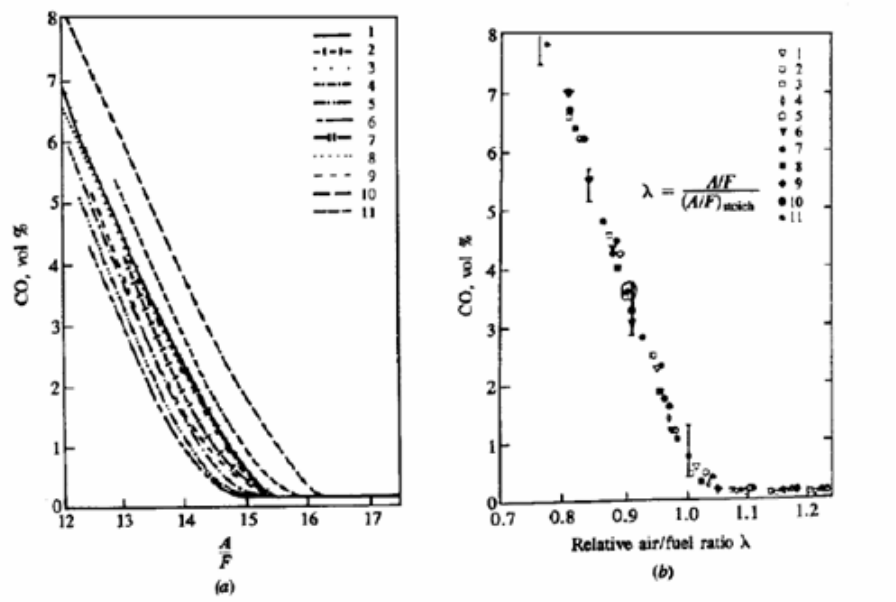

Figure 2: Variation of SI engine CO emissions with eleven fuels of different H/C ratio. (a) with air/fuel ratio; (b) with relative air/fuel ratio λ

The Figure (2) show the CO emissions of a spark ignition engine, the engine is fuelled with 11 different fuels (different respect to the H/C ratio), in function to α (air/fuel ratio) and λ (α/α_{st}).

In the graph it can be observed that CO concentrations measured at the engine exhaust depend almost exclusively from the A/F ratio, with rapidly increasing CO concentration values in the rich region as A/F is decreased. At the same time, for leanest mixtures still appears a certain quantity of CO concentrations.

Finally, it can be noticed that all the fuel rich operating conditions (cold start, acceleration transients, and full load) as well as A/F ratio imbalances from cylinder to cylinder will cause significant increases in CO emissions.

1.2.2 *Hydrocarbons HC*

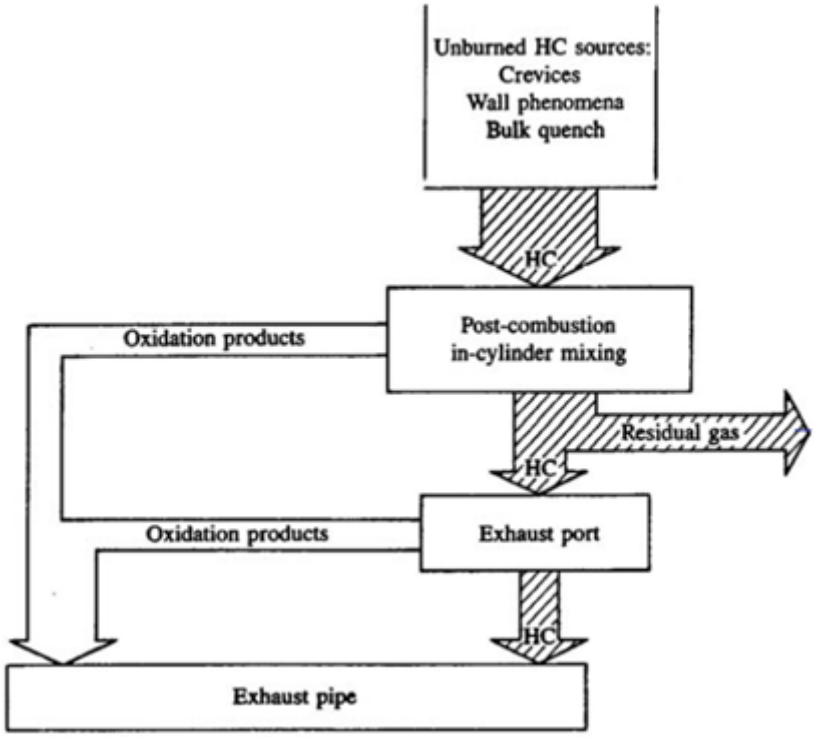

Figure 3: Schematic of complete SI engine HC formation and oxidation mechanism within the cylinder and exhaust system

The above Fig. (3) shows a scheme of the HC formation mechanism. In the first part, up to about 9 % of the fuel is not involved in the main combustion process; between 50 – 80 % of unburned HC is oxidized still in the cylinder; around 40 % of HC exhausted is oxidized in the exhaust port and 1-2% of the fuel is exhausted at the tailpipe.

However, despite the apparent high level of combustion efficiency, these relatively low emission levels are mainly due to post-flame oxidation reactions that take place both into the cylinder and in the exhaust ports.

Although postflame oxidation are effective in reducing HC emissions, the efficiency of the engine is markedly affected, since the chemical energy of the fuel is converted into exhaust gases enthalpy instead of being converted into piston work.

Less than 50% of HC are made of unburned fuel: most of unburned hydrocarbons are instead constituted by partial oxidation

products and pyrolysis products, which are usually extremely reactive for photochemical smog reactions (secondary pollutants).

The main HC formation mechanisms in spark ignition engines are the followings:

- Mixture trapped into crevice volumes (crevices 30-60% of total HC for a warmed up engine)
- Fuel trapped into the oil layer (oil layer 5-30% of total HC for a warmed up engine)
- Flame quenching at the combustion chamber walls (wall quenching 5-20 % of total HC)
- Bulk quenching or incomplete combustion (bulk quenching - usually significant only for $\lambda \gg 1$ or EGR $\uparrow\uparrow$)
- Fuel trapped by deposits (deposits 0-25% of total HC)

1.2.2.1 *Mixture trapped into crevice volumes (crevices 30-60% of total HC for a warmed up engine)*

During compression, as pressure rises, part of the mixture is forced to enter into the combustion chamber crevices (e.g. the volume between piston, liner and rings, the head gasket crevice, etc.), where the flame front cannot propagate. Later, during the expansion stroke, when in the main combustion chamber the pressure drops below the pressure level into the crevices, the trapped mass flows back into the cylinder, but cannot complete its oxidation process.

As the engine temperature increases, the “ring pack” volume diminishes significantly, diminish (up to the 30% less) due to clearances decrease.

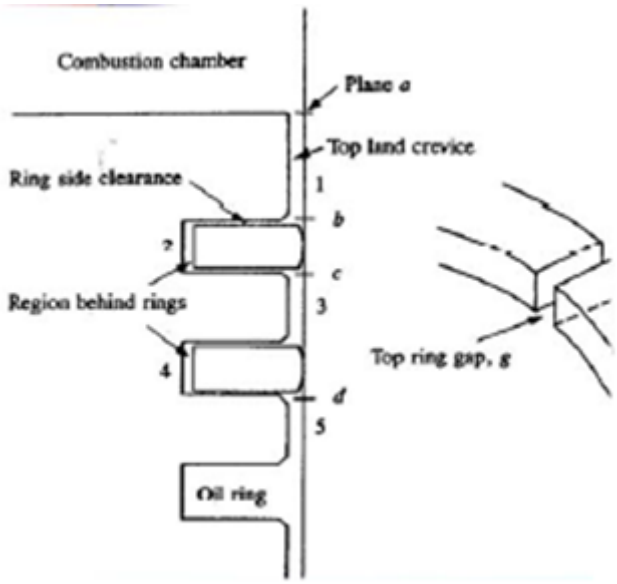

Figure 4: Schematic representation of the ring pack

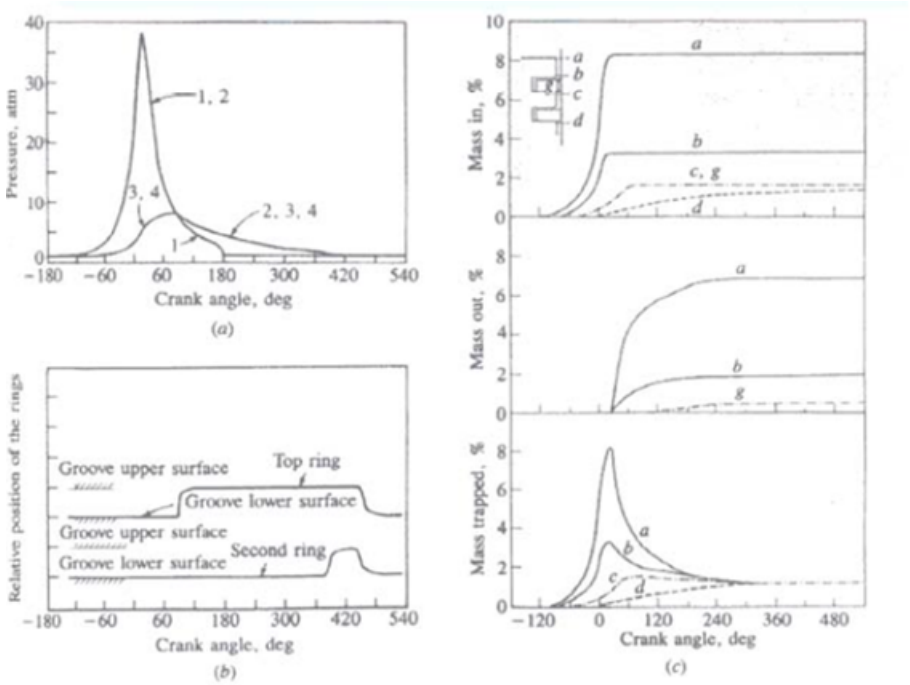

Figure 5: (a) Pressures in the combustion chamber (1), in region behind top ring (2), in region between rings (3), and behind the second ring (4); (b) relative position of top and second rings; (c) percentage of total cylinder mass that flows into and out of the different crevice regions across planes a,b,c and d and through the ring gap g in Fig. 4, and the percentage of mass trapped beneath these planes, as a function of crank angle. Automotive spark-ignition engine at wide-open throttle and 2000 rpm

In the figures (4) and (5), are represent different zones on the "ring pack", specifically in the Fig. 4 is show the pressure distribution, the mass trapped and the relative position of the rings.

The "ring pack" volume is the major responsible for crevice related HC. Even if the ring pack volume can represent about 2% of the clearance volume, due to the high density of the cool mixture it may trap up to 10% of the in cylinder mass.

The engine blow-by allow decrease the HC emissions, since the gas trapped into the "ring pack" can be in taken again by the engine.

1.2.2.2 *Fuel trapped into the oil layer (oil layer 5-30% of total HC for a warmed up engine)*

Fuel vapor can be absorbed by the oil layer on the cylinder liner during the compression stroke, when the fuel partial pressure is high.

Afterward, during the expansion stroke, when the fuel partial pressure drops because fuel species are removed from the gas mixture by the combustion process, the oil layer desorbs the hydrocarbon molecules that were previously trapped, but at that time they are unable to complete their oxidation process.

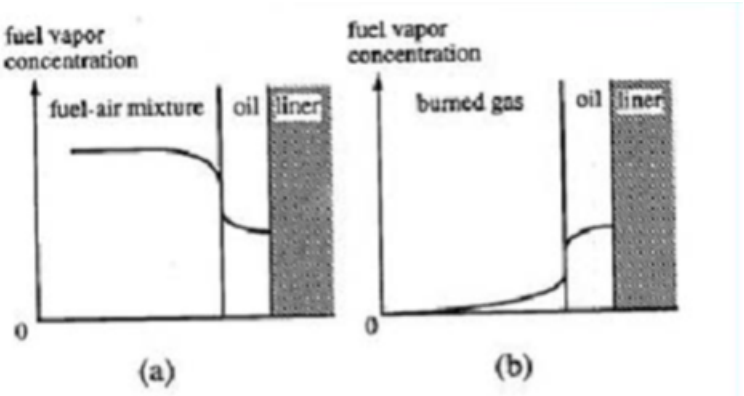

Figure 6: Schematic of oil layer mechanism. Gasoline component vapor concentration profile in the gas and in the oil layer on the cylinder liner; (a) during compression; (b) during expansion

Another phenomenon that affects the fuel trapped into the oil layer is the solubility and depending on the fuel molecule characteristics (it increases with the molecular weight of the hydrocarbon

molecule, being negligible for light gas molecules such as methane or propane), and is significantly affected by the temperature (the lower the oil temperature, the higher the solubility).

1.2.2.3 *Flame quenching at the combustion chamber walls (wall quenching 5-20 % of total HC)*

The flame front usually quenches before reaching the combustion chamber walls, due to the presence of a thermal boundary layer in which mixture temperature is close to the walls temperature (e.g. about $400°K$ on the liner), and therefore too low for the oxidation reactions.

The thickness of this thermal boundary layer may vary in a range between 0.04-0.2 mm, and is inversely proportional to in-cylinder pressure.

This mechanism is therefore gaining more relevance at part load. When two cold walls are facing each other the minimum distance between the two walls that allows the flame front propagation is roughly 5 times higher than the thermal layer thickness on a single wall, i.e. 0.2-1 mm are the minimum values of the crevice region in which the flame can propagate.

1.2.2.4 *Bulk quenching or incomplete combustion (bulk quenching – usually significant only for $\lambda \gg 1$ or EGR $\uparrow\uparrow$)*

Bulk quenching is less likely to happen if the combustion process is fast.

1.2.2.5 *Fuel trapped by deposits (deposits 0-25% of total HC)*

- *Deposits on the intake valve*: they absorb fuel during the acceleration transients, and they then release fuel during deceleration phases, causing mixture enleanment during tip-in and enrichment during tip-out, and thus increasing HC emissions during transients.
- *Deposits on the combustion chamber walls*: they can trap and release fuel with a mechanism similar to that of the oil layer, thus leading to an increase of HC emissions with engine

age. However, they can fill part of the crevice volumes, and reduce the heat exchange between the gases and the walls, thus increasing the combustion temperatures and leading to a decrease of HC emissions as deposits build up with engine aging.

- *Liquid fuel fractions at cold start*: during cold start HC emissions rise significantly due to incomplete fuel evaporation. Usually in PFI engines the fuel injection takes place when the intake valve are closed, thus allowing a good fuel vaporization before the intake stroke, since fuel is heated up by the hot valve stem and back plate as well as by the mixing with hot residual gases that flow back into the exhaust port at intake valve opening.

However at cold start a high fraction of the fuel is unable to vaporize, thus requiring the use of mixture enrichment in order to be able to obtain a close to stoichiometric mixture with the more volatile fraction of the fuel.

HC emissions at cold start may therefore increase up to 50% for an engine starting at 0°C.

1.2.3 *Nitric oxide NO*

The concentrations of the pollutants measured at engine exhaust are different from values calculated assuming chemical equilibrium, since chemical reactions kinetics play a fundamental role.

For some pollutants such as CO, HC and PM, the formation and destruction processes are intimately coupled with the fuel combustion processes, and thus the understanding of their formation mechanisms requires the understanding of the combustion chemistry.

For other pollutants such as NOx, although the formation and destruction processes are not part of the fuel combustion processes, the reactions that produce these species take place in an environment which is the result of the combustion reactions, so that once more the understanding of the combustion chemistry is extremely important.

Nitric oxide (NO) forms throughout the high temperature burned gas behind the flame front, due to oxidation reactions of nitrogen

that occur at high temperature (above $1850°K$), without attaining chemical equilibrium (thermal NOx).

The higher the burned gas temperature, the higher will be the NO formation rate.

Afterward, during the expansion stroke, as burned gases cool down, chemical reactions involving NO formation and destruction freeze, leaving NO concentrations far above the levels corresponding to chemical equilibrium at exhaust conditions.

In spark ignition engines most of NOx are constituted by NO (about 98-99%), while NO_2 share is small (about 1-2%). The main reactions leading to NO formation are the following, according to the oxidation mechanism proposed by Zeldovich (thermal NOx formation):

1. $O + N_2 \rightarrow NO + N$
2. $N + O_2 \rightarrow NO + O$
3. $N + OH \rightarrow NO + H$

Reaction n.(1) has a very high activation energy that causes a high sensitivity to temperature: the process can therefore start only in the burned gas region.

The N atoms that form from reaction n.(1) is unstable, and can therefore react with oxygen, forming NO and O (reaction n.(2)). Finally, according to reaction n.(3), OH radicals can also react with Nitrogen, to form NO and hydrogen. Mixture burning at the beginning of the combustion process is further compressed after combustion reaching higher temperatures. Mixture burning later is compressed mainly before burning, and reaches lower temperatures. Therefore the earlier burning fraction contributes more to NO formation, and frozen NO concentrations in the early burning fractions can be an order of magnitude higher than concentrations in the late burning fractions.

1.2.3.1 *Prompt formation mechanism*

$$CH + N_2 \rightarrow HCN + N$$

Although the thermal formation process of NO previously described is the main responsible of NO formation in SI engines, the so called prompt mechanism can have some importance, especially for low temperature combustion conditions.

The nitrogen molecule can be broken, involving CH radicals in the process to form HCN and N, that can then both react with oxygen to form NO.

This mechanism takes places inside the flame front, where HC concentrations are high, and is extremely fast, with a reduced sensitivity to temperature, since the activation energy is low.

1.3 EXHAUST GAS RECIRCULATION (EGR)

Exhaust gas recirculation is an emission control technology, by which a portion of engine's exhaust gas is returned to the combustion chambers via the inlet system in order to reduce NOx emissions, thanks to a substantial decrease in the peak temperature of the diesel combustion flame. [2]

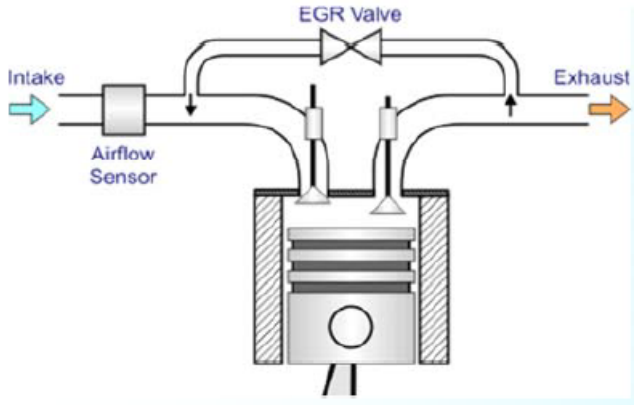

Figure 7: Schematic representation of the EGR circuit

In engine evolution, the Exhaust Gas Recycle (EGR) technique was firstly adopted in diesel engines in order to limit the thermal NO,. formation rate by limiting the combustion chamber temperature thanks to the dilution of the fresh charge with a certain amount of exhaust gases recycled at the engine intake. Today, EGR is commonly used also in spark-ignition engines since this technique is able to both limit the NO formation rate and improve engine thermodynamics at some operating points. EGR in

fact, decreases pumping losses at partial load, while improves the detonation resistance at full load operation. Many times, EGR is obtained by means of a re-aspiration of the exhaust gases through the exhaust valve thanks to a variable valve timing (internal EGR), rather than realizing an appropriate circuit from the exhaust to the intake port (external EGR). [3]

1.3.1 *Definition of exhaust gas recirculation percent.*

The percent of exhaust gas recirculation (EGR(%)) is defined as the percent of the total intake mixture which is recycled exhaust, [4]

$$EGR_{\%} = \frac{m_{EGR}}{m_i} x100 \tag{1}$$

where $m_i = m_a + m_f + m_{EGR}$ and m_{EGR} is the mass of EGR. Up to about 30% of the exhaust can be recirculated.

An alternative definition of percent EGR is also used, based on the ratio of EGR to fresh mixture (fuel and air):

$$EGR_{\%} = \left(\frac{m_{EGR}}{m_a + m_f} \right) x100 \tag{2}$$

The EGR ratio also, in some cases is defined as the volumetric ratio of the recirculated gas to the total charge induced into the cylinder. In such cases, the EGR ratio can reach 50%.

$$EGR_{\%} = \frac{V_{EGR}}{V_{air} + V_f + V_{EGR}} x100 \tag{3}$$

1.3.2 *EGR configurations*

The EGR can be applied through different configurations:

- External EGR
  - High Pressure Loop (Short Route) EGR.
  - Low Pressure Loop (Long Route) EGR.
  - Dual Loop or Mixed Loop EGR.
- Internal EGR
  - Pre-opening of the Intake valve.
  - Post opening of the Exhaust valve.

1.3.2.1 *High pressure EGR*

The EGR is passed from upstream of the turbine to downstream of the compressor. [5]. EGR cooling is applied in all but the most basic applications to promote further NOx and particulate reductions.

A pressure gradient between the exhaust and intake manifolds is required to drive EGR. This is an important consideration for turbocharger matching. VGT and inlet throttles are often included in these systems to increase pressure gradient across the engine at certain operating conditions (notably low engine speeds and loads). [6]

Figure 8: Schematic representation of the High Pressure EGR configuration

1. Advantages
    a) Simple configuration.
    b) Compatible with the today engine / vehicle layout solution.
    c) Fast transient response.
2. Drawbacks
    a) EGR cooling capability / turbocharger efficiency.

1.3.2.2 *Low pressure EGR*

Before the market introduction of Diesel particulate filter (DPF), the entire air intake system including the compressor would have been subject to deposit formation. This was one of the main reasons that limited the application of this kind of system. The DPF can be therefore seen as enabler of LP EGR [7].

The passage for EGR is provided from downstream of the turbine to the upstream side of the compressor. The entire exhaust gas volume passes through the turbine, DOC (diesel oxidation catalyst) and the DPF (diesel particle filter) then the EGR gas is extracted from the exhaust stream and aspirated by the compressor along with the fresh air. The EGR gas is therefore at a lower pressure when it is combined with the fresh air than in the high pressure EGR circuit [8].

Below are the advantages and disadvantages of this system:

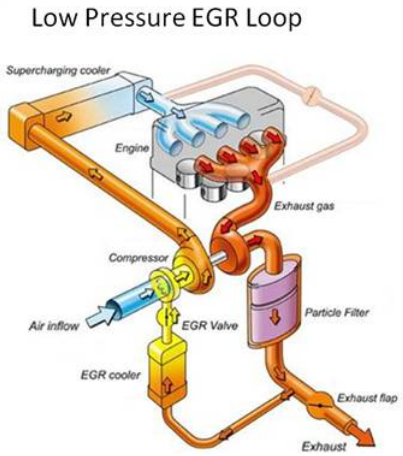

Figure 9: Schematic representation of the Low Pressure EGR configuration

1. Advantages

    a) Clean EGR.

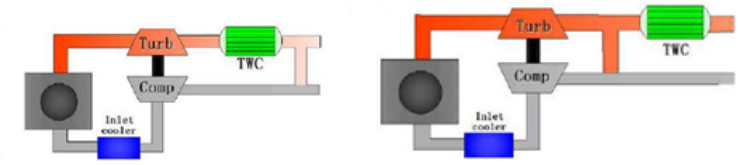

(a) Clean (b) Dirty

Figure 10: Schematic representation of the both systems.

    b) Significant cooling efficiency (very low intake manifold temperature).

    c) Better turbo efficiency (turbo response independent from EGR rate), i.e, more energy available to the turbine to power the compressor, so higher EGR rates may be attained compared to high pressure EGR.

2. Drawbacks

    a) Transient response.

    b) Additional exhaust flow could cause a more rapid loading of the DPF if the engine-out particle emissions are not reduced.

    c) Compressor damage by water droplets and particles from exhaust components.

    d) Acidic condensation in the EGR cooler and the charge air cooler.

1.3.2.3 *Dual loop EGR system*

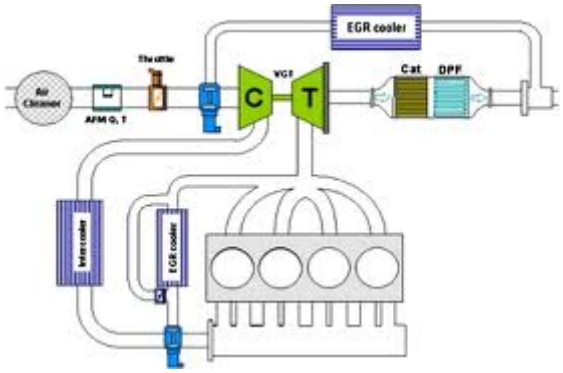

Figure 11: Schematic representation of the Dual Loop EGR system

The integration of the two systems is useful in order to try to combine the advantages of both. In particular the short route EGR is used during the warm up phases and when high transient response is required.

Conventional control strategy for both system HP and LP EGR:

1. The ECU sets the VGT position according to a boost target.
2. The air flow meter measures the intake Mass Air Flow (MAF).
3. The ECU compares the actual MAF value with a target value which has been set up for each engine operating condition.
4. The ECU actuates the EGR valve trying to reach the target MAF value.

1.3.2.4 *Control and limitations*

A control strategy is needed for the following actuators:

- EGR valve (used to control EGR flow).
- VGT actuator (used to control the boost level).

Limits to max EGR rate

When high EGR rates are necessary the pressure difference $\triangle$p between the exhaust and intake manifold could not be high enough. Various strategies have been used to increase $\triangle$p:

- Intake throttling (as commonly used in light-duty diesel engines).
- Use of a venturi (more common in heavy-duty engines), more efficient (less fuel economy penalty) compared to exhaust throttling. Moreover proper design of the venturi device can also enhance mixing of EGR with the fresh air, resulting in better EGR distribution between engine cylinders.

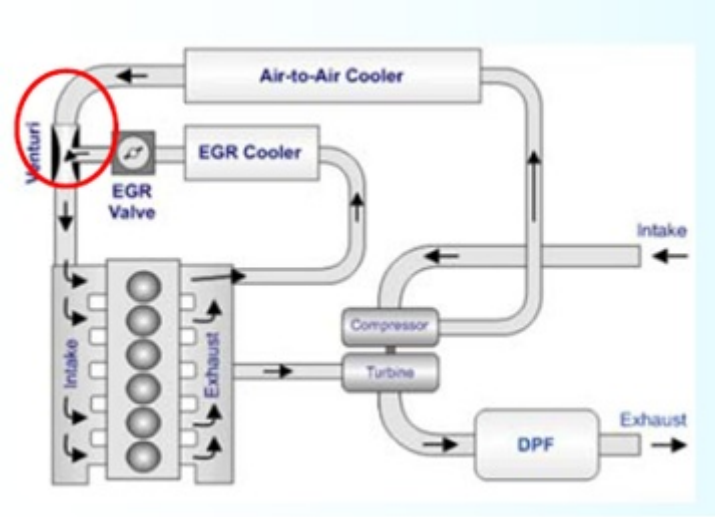

Figure 12: Schematic representation of the High Pressure EGR configuration using the venturi solution to increase the differential pressure

Advantages of the Low Pressure Loop EGR system include (besides the better soot/NOx trade-off):

1. Lower fuel consumption than the HPL configuration as a result of better turbocharger performance.
2. With the presence of a particulate filter, the LPL EGR supplies predominantly filtered exhaust to the inlet of the engine through the turbocharger compressor. Therefore, engine durability can be better preserved.
3. Exhaust gas downstream of the particulate filter is cooler than that provided from upstream of the turbocharger (as in the HPL case): an opportunity exists to reduce EGR cooling requirements (reduced size EGR cooler) and provide a more compact unit. In addition, the EGR cooler would have less heat rejected in the engine water jacket and therefore, less cooling load for the radiator to handle.

4. Better EGR and fresh charge air mixing resulting from introducing the mixture upstream of the turbocharger compressor.

However, the LPL EGR system has not been favored over the HPL system for a number of reasons described as follows:

1. Even though LPL EGR is sourced downstream from the particulate filter, it is not entirely free from carbonaceous material, since the filter trapping efficiency is less than 100 percent. With carbonaceous material still remaining in the recirculated exhaust stream, its impaction on the compressor wheel as it turns at a high rate of speed may potentially erode the wheel, which therefore will need special machining and surface treatment.

2. In cases where air-to-air intercoolers are used, carbonaceous and other unfiltered matter flowing through the compressor would likely be trapped in the narrow cooler passages. If left to accumulate over time, air flow to the engine would be reduced, leading to performance as well as emission and fuel economy deterioration.

3. Plumbing for the LPL EGR arrangement is often awkward and cumbersome. Water vapor contained in the exhaust may condensate inside the aftercooler, leading to acidic corrosion.

1.3.2.5 *Internal EGR*

EGR strategy performed acting on the valve control that is called MultiAir. Different valve opening and closing strategies are employed to optimize the efficiency of combustion. The strategies to command the intake valves, at this moment for the MultiAir system with a solenoid valve by cylinder are four: ϕ_1 (Late Closening), ϕ_2 (Early Opening), MultiLift (ML), and Full lift (FL). [9]

At Figure (13) are shown the different intake valve lifts, according to the implemented strategy.

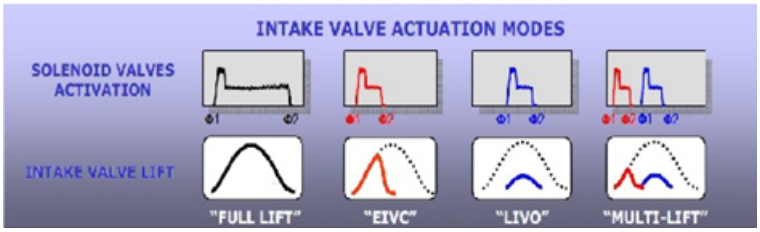

Figure 13: Intake Valve Actuation Modes

- Complete valve opening, known as "Full Lift'', the current mode of conventional engines, is used by MultiAir, only when full engine power is required, for instance, on highways. Keep the high pressure chamber in its closing state, and therefore the intake valves completely follow the camshaft imposed profile. The camshafts are optimized to the full power, and the closing postponement is changed to obtain the maximum mean effective pressure (MEP) for each speed.

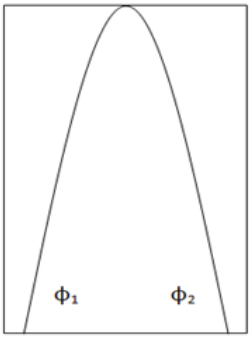

Figure 14: Full Lift Mode

ϕ_1: Maximum value to guarantee a full-lift regulation

ϕ_2: Minimum value to guarantee a full-lift regulation

- *Late Opening:* is a post-opening of the intake valve. At engine partial load, during engine start up and idling, LIVO (Late Intake Valve Opening) optimizes the valve opening delivering the correct air/ fuel mixture for combustion.

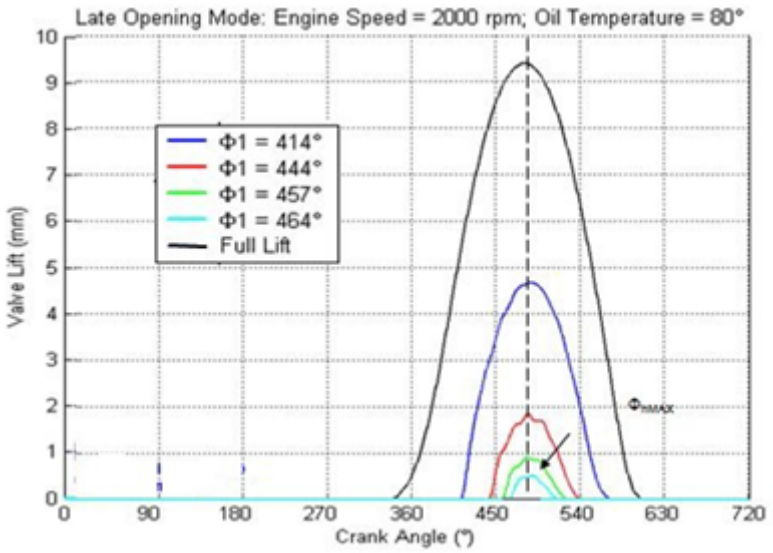

Figure 15: Valve Lift (mm) vs Crank Angle (°). The angle $\phi 1$ is the controllable intake valve opening angle. $\phi 2$ not controllable intake valve closing angle.

This strategy is used with very low loads and the speed operation points, where, would not be possible to obtain a stable ignition using thorough early closing angles, due to, the reduced ratio of the effective combustion.

- *Early Closening*: is a pre-closening of the intake valve. At medium-low rpm torques and for engine full load, EIVC (Early Intake Valve Closing) optimizes volume efficiency and reduces pumping losses. Undesired back flow into the manifold is avoided and air mass in the cylinder optimized, e.g. during acceleration.

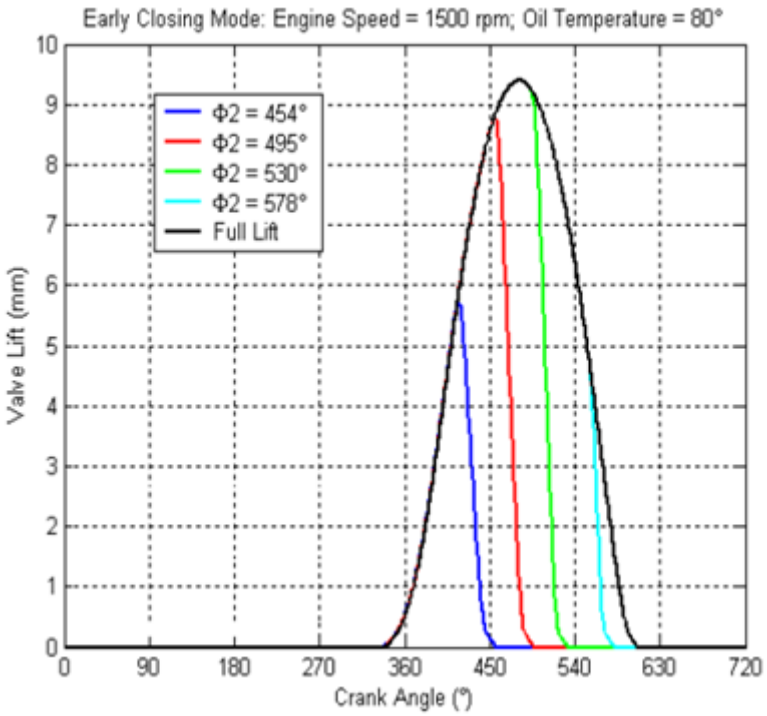

Figure 16: Valve Lift (mm) vs Crank Angle (°). The angle $\phi 2$ is the controllable intake valve closing angle

The intake valves with the ϕ_2 mode, at the starting of the intake phase, follow the profile imposed by the cam. The valve lift continue until the ECU commands the valve closing of the MultiAir System; in this way, it is obtained a lower lift respect to the Full lift Mode (when the closing takes place before the physical angle of the cam's maximum lift) and an angularly early valve closing.

- *Multilift*: is a mode that has two consecutive lifts, the first in ϕ_2 mode and the second in ϕ_1 mode, interspersed with a very short time interval. With this strategy two lifts are obtained, both lower than those achievable in Full Lift.

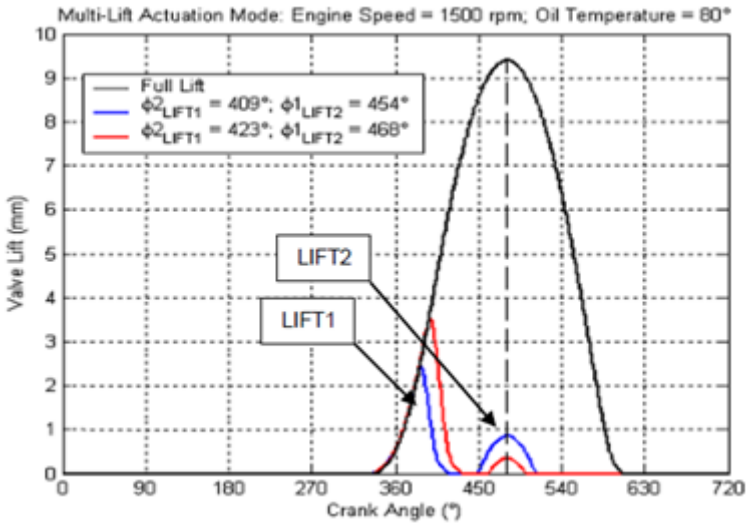

Figure 17: Valve Lift (mm) vs Crank Angle (°). In the graph: ϕ_{1Lift1} is not controllable intake valve opening angle (driven by cam and oil compressibility); ϕ_{2Lift1} is controllable intake valve closing angle (used for charge control); ϕ_{1Lift2} is controllable intake valve opening angle for second lift (used for combustion control) and ϕ_{2Lift2} is not controllable intake valve closing angle for second lift (driven by cam and oil hydraulic circuit)

Multilift can be considered the most generic valve actuation. The late opening and early closing parts are two subsets which can be chosen using Air Fraction.

The Air Fraction indicates the percentage of target air which has to flow into the cylinder between early closing or late opening actuation valve lifts.

- ϕ_1: air fraction 100%
- Multi-Lift (ML): air fraction between 0 e 100%
- ϕ_2: air fraction 0%

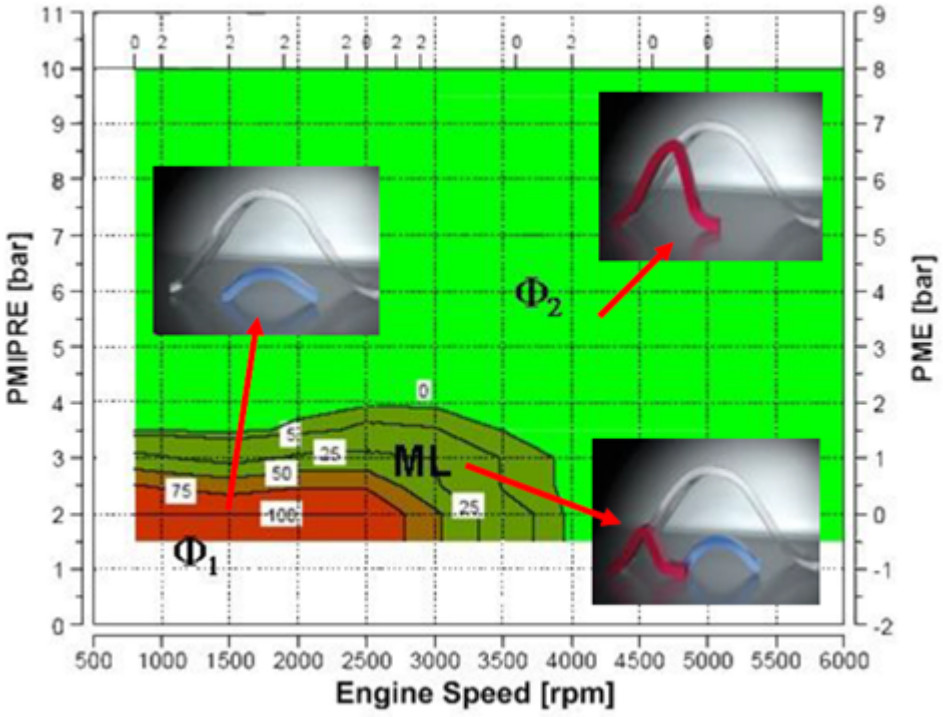

Figure 18: Different VVA modes depending on engine operating conditions

1.4 EGR IN PFI ENGINES AND IN GDI ENGINES

1.4.1 *PFI engines*

PFI engines work under stoichiometric condition, and EGR is employed primarily to reduce throttling loss at part load range, thus to reduce fuel consumption, the addition of EGR resulted in higher fuel consumption benefits of 10-20%. Furthermore, lower exhaust gas temperatures can be reached thus avoiding damages to the noble metals of catalytic converters [3]. In second place, EGR allow to reduce NOx emission levels.

In order to keep the same torque and power output after introducing EGR in gasoline engine, further opening of engine throttle is necessary to raise the trapped charge density. This can reduce pumping loss and improvement of fuel economy compared with that when no EGR is used.

The improvement in fuel consumption with increasing EGR is due to three factors:

- First, reduced pumping work, as EGR increases at constant brake load (fuel and air flows remain almost constant, hence, intake pressure increases).
- Second, reduced loss of heat transferred to cylinder wall since burned gas temperature is decreased significantly.
- Third, a reduction in the degree of dissociation in the high temperature burned gases [4], which allows more fuel's chemical energy to be converted to sensible energy near TDC.

It is worth to mention that when PFI engine works at full load, the throttle has reached the WOT condition. In this case, the throttle cannot be opened more to increase intake density. Therefore, boosting intake pressure is necessary to gain the same level of torque and power output. If supercharge is not used to increase intake density, the power loss will increase with the increase of EGR ratio at full load. Furthermore, in a conventional PFI engine, EGR trends to influence combustion stability and investigations have confirmed that both ignition delay and combustion period are extended with EGR due to the associated decrease in laminar flame speed. Consequently, it may be appropriate to use EGR in combination with other techniques [10].

1.4.2 *GDI engines*

In general, a larger NOx reduction can be realized with EGR in GDI engines than in either PFI engines or diesel engines. For GDI engines, the available fuel-air mixing time is comparatively longer than diesel engines, and, as a result EGR role is more effective and NOx emission can be further reduced. In a GDI engine, since there is no throttling effect, the engine works with lean or even ultra-lean mixtures and the in-cylinder A/F is higher and the introduction of exhaust gas replaces part of fresh air directly. For a given torque and power output, the amount of fuel that engine supplies must be constant. Therefore, the in-cylinder air fuel ratio decreases with the increment of the exhaust gas, which can reduce NOx emission effectively. Although in GDI engine, lean-NOx aftertreatment technologies can be used to reduce NOx emission, EGR was considered the only feasible way to reduce NOx. In addition, EGR ratio as high as possible are required to keep GDI engine working under stoichiometric condition, so that TWC can work normally, and then can use it to reduce HC and CO emission.

Experiments in GDI shows [11] that at low and part load the NO and CO emissions decrease and a reduction of fuel consumption by up to 4%, primarily through the reduction in pumping losses. At high loads, the addition of EGR resulted in higher fuel consumption benefits of 10-20% as well as the expected NO and CO reductions. The fuel economy benefit at high loads resulted from a decrease in knock tendency and a subsequent improvement in combustion phasing as well as reductions in exhaust temperatures that eliminated the requirement for over-fuelling.

When EGR is used in GDI engine, providing appropriate amount of EGR has always been a design challenge, since a relative higher EGR mass flow rate must be metered and the flow must be distributed uniformly to individual cylinders under a much lower pressure difference with that of traditional PFI engines. The flow of so much EGR may require a moderate level of intake vacuum, which will cause great pumping loss, while GDI engines is supposed to reduce such loss substantially.

Naturally, the EGR adoption modifies engine combustion characteristics: the charge dilution slows down the flame front propagation rate but increases the end gas autoignition time (improve the knock resistance). Since exhaust gases reach lower temperature levels, mixture enrichment is no more necessary in order to cool them. In this way, damages to the exhaust turbine and the noble metals of catalytic converters can be avoided.

One of the disadvantages of the use of EGR in gasoline engines is the reduction in the volumetric efficiency, hence in torque delivered, a solution for this could be to increase the boost pressure in order to compensate the losses in volumetric efficiency. Furthermore, an excessive amount of recycled exhaust could lead to very low combustion rates, thus unstable combustion could occur, a large cycle by cycle variation, deterioration in car drivability and an increasing pollutant formation could appear [3].

1.5 FLOW PAST THROTTLE PLATE

This section will describe the characteristics of the throttle plate located in the manifold that is in charge to introduce the fresh air + EGR into the cylinders, as this throttle plate has the same configuration than the EGR throttle plate, all the different concepts could be applied to the case in study.

Except at or close to wide-open throttle, the throttle provides the minimum flow area in the entire intake system. Under typical road-load conditions, more than 90 percent of the total pressure loss occurs across the throttle plate. The minimum-to-maximum flow area ratio is large-typically of order 100. Throttle plate geometry and parameters are illustrated in Figure (19). A throttle plate of conventional design such as Fig. (19) create a three-dimensional flow field. At part-throttle operating conditions the throttle plate angle is in the 20° to 45° range and jets issue form the "crescent moon" shaped open areas on the either side of the throttle plate. The jets are primarily two dimensional. Figure (20) shows photographs taken of a two-dimensional hydraulic analog of a typical carburetor venturi and throttle plate in steady flow at different throttle angles. The path lines traced by the particles in the flow indicate the relative magnitude of the flow velocity. The flow accelerates through the carburetor venturi (separation occurs at the corners of the entrance section); it then divides on either side of the throttle plate. There is a stagnation point on the upstream side of he throttle plate. The wake of the throttle plate contains two vortexes which rotate in opposite directions. The jets on either side of the wake (at part throttle) are at or near sonic velocity. There is little or no mixing between the two jets. Thus, if wrong distribution of the fuel-air mixture occurs above the throttle plate, it is not corrected immediately below the throttle plate. [1]

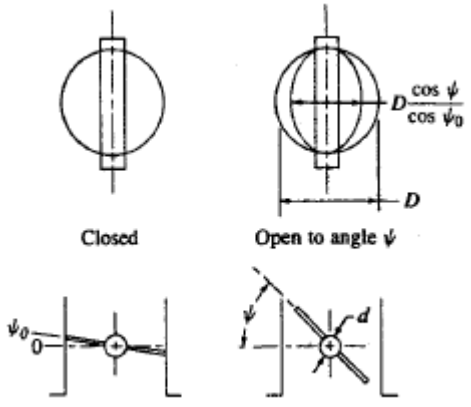

Figure 19: Throttle plate geometry

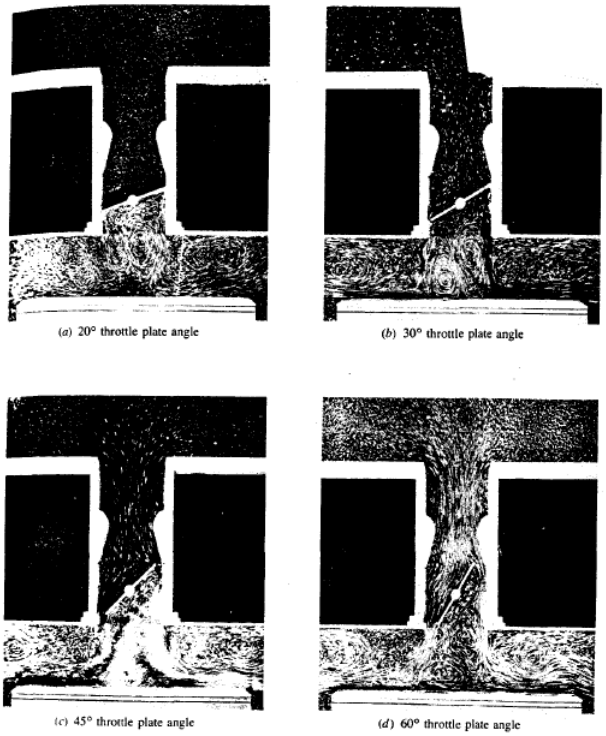

Figure 20: Photographs of flow in two-dimensional hydraulic analog of carburetor venturi, throttle plate, and manifold plenum floor at different throttle plate angles

In analyzing the flow through the throttle plate, the following factors should be considered:

1. The throttle plate shaft is usually of sufficient size to affect the throttle open area.

2. To prevent binding in the throttle bore, the throttle plate is usually completely closed at some nonzero angle (5,10, or 15°).

3. The discharge coefficient of the throttle plate is less than the a smooth converging-diverging nozzle, and varies with throttle angle, pressure ratio, and throttle plate Reynolds number.

4. Due to the manufacturing tolerances involved, there is usually some minimum leakage area even when the throttle plate is closed against the throttle bore. This leakage area can be significant at small throttle openings.

5. The measured pressure drop across the throttle depends (±10 percent) on the circumferential location of the downstream pressure tap.

6. The pressure loss across the throttle plate under the actual flow conditions (which are unsteady even when the engine speed and load are constant) may be less than under steady flow conditions.

The throttle plate open area A_{th} as a function of angle ψ for the geometry in Fig. (19), is given by:

$$\frac{4A_{th}}{\pi D^2} = \left(1 - \frac{cos\psi}{cos\psi_0}\right) + \frac{2}{\pi}\left[\frac{a}{cos\psi}\left(cos^2\psi - a^2cos^2\psi_0\right)^{\frac{1}{2}}\right] -$$

$$\frac{2}{\pi}\left[a\left(1-a^2\right)^{\frac{1}{2}} + sin^{-1}a - \frac{cos\psi}{cos\psi_0}sin^{-1}\left(\frac{acos\psi_0}{cos\psi}\right)\right] \quad (4)$$

where $a = \frac{d}{D}$, d is the throttle shaft diameter, D is the throttle bore diameter. andψ_0 is the throttle plate angle when tightly closed against the throttle bore. When $\psi = cos^{-1}(acos\psi_0)$, the throttle open area reaches its maximum value ($\approx \pi D^2/4 - dD$). The throttle plate discharge coefficient (which varies with A_{th} and minimum leakage area, must be determined experimentally.

The mass flow rate through the throttle valve can be calculated from standard orifice equations for compressible fluid flow.

For pressure ratios across the throttle greater than the critical value ($\frac{p_T}{p_0} = 0.528$), the mass flow rate is given by:

$$\dot{m}_{th} = \frac{C_D A_{th} p_0}{\sqrt{RT_0}}\left(\frac{p_T}{p_0}\right)^{\frac{1}{\gamma}}\left\{\frac{2\gamma}{\gamma-1}\left[1 - \left(\frac{p_T}{p_0}\right)^{\frac{(\gamma-1)}{\gamma}}\right]\right\}^{\frac{1}{2}} \quad (5)$$

where A_{th} is the throttle plate open area (Eq. 4), p_o and T_0 are the upstream pressure and temperature, p_T is the pressure downstream of the throttle plate (assumed equal to the pressure

at the minimum area: i.e., no pressure recovery occurs), and C_D is the discharge coefficient (determined experimentally).

For pressure ratios less than the critical ratio, when the flow at the throttle plate is choked,

$$\dot{m}_{th} = \frac{C_D A_{th} p_0}{\sqrt{RT_0}} \gamma^{\frac{1}{2}} \left(\frac{2}{\gamma+1}\right)^{\frac{(\gamma+1)}{2(\gamma-1)}} \tag{6}$$

The relation between air flow rate, throttle angle, intake manifold pressure and engine speed for a two-barrel carburetor and a 4.7 dm^3 (288in^3) displacement eight-cylinder production engine is shown in Fig. (21). While the lines are predictions from a quasi-steady computer simulation, the agreement with data is excellent. The figure shows that for an intake manifold pressure below the critical value (0.528 x p_{atm} = 53.5 kN/m^2 = 40.1 $cmHg$) the air flow rate at a given throttle position is independent of manifold pressure and engine speed because the flow at the throttle plate is choked.

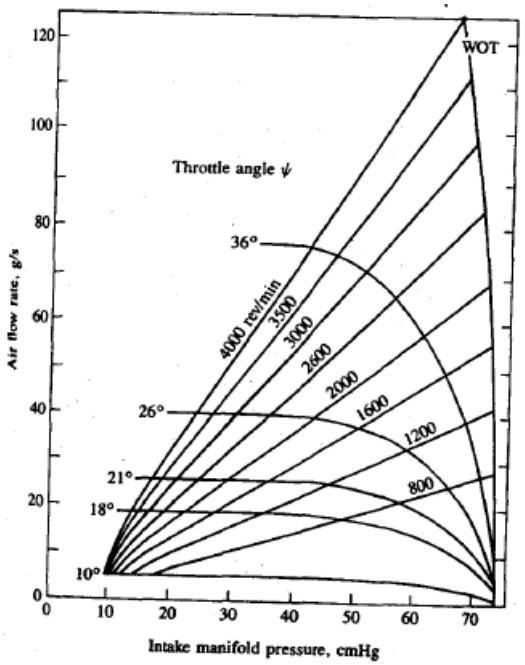

Figure 21: Variation in air flow rate past a throttle, with inlet manifold pressure, throttle angle, and engine speed. 4.7dm^3 displacement eight-cylinder engine

2

SOFTWARE USED FOR DEVELOP THE MODEL

In this thesis, the software that used is Matlab, and specifically Simulink, that allow the implementation of an internal tool develop by CRF FPT that is adapted to the different needs of the Multiair group.

2.1 MATLAB AND SIMULINK

MATLAB (matrix laboratory) is a numerical computing environment, developed by MathWorks; MATLAB allows matrix manipulations, plotting of functions and data, implementation of algorithms, creation of user interfaces, and interfacing with programs written in other languages, including C, C++, Java, and Fortran.

An additional package, Simulink, adds graphical multi-domain simulation and Model-Based Design for dynamic and embedded systems. Simulink is a tool for modeling, simulating and analyzing multidomain dynamic systems. Its primary interface is a graphical block diagramming tool and a customizable set of block libraries. It offers tight integration with the rest of the MATLAB environment and can either drive MATLAB or be scripted from it. Simulink is widely used in control theory and digital signal processing for multidomain simulation and Model-Based Design. [12]

The Simulink simulation environment has the following properties:

- Libraries of predefined blocks expandable to custom blocks.
- Interactive graphical editor for assembling and managing the block diagrams.
- Ability to manage complex projects by dividing the models into hierarchies of components.

- Tool Model Explorer to navigate, create, configure, and search all signals, parameters, properties, and the generated code associated with a model.

- APIs (application programming interfaces) enabling connections to other simulation programs and allow you to include manually written code.

- Embedded MATLAB function block in Simulink to import MATLAB algorithms and implementations in embedded.

- Simulation modes (Normal, Accelerator and Rapid Accelerator) for running simulations so interpreted, or the speed of compiled C code solvers with fixed or variable.

- Graphics debugger and profiles to examine simulation results and diagnose performance problems and unexpected behavior of the project.

- Full access to MATLAB for analysis and visualization of the results, to customize the modeling environment and define signals, parameters and test.

- Analysis tools and diagnostics to ensure the consistency of the model and identify potential errors.

2.1.1 *Creating and using the models*

Simulink allows you to create, model quickly and maintain a detailed block diagram of the system, through the use of a set of predefined blocks; provides tools for modeling hierarchical data management and customization of the subsystems to facilitate the creation effective representations of the system. The software includes a library of functional blocks commonly used in modeling a system. Among them:

- Dynamic Blocks continuous and discrete, such as Integration and Unit Delay.

- Algorithmic blocks, such as Sum, Product and Lookup Table.

- Building blocks, such as Mux, Selector Switch and Bus.

Others extend the functionality of Simulink blockset for specific applications, such as aerospace, communications, radio frequency, signal processing, video and images, and more. In Simulink it is possible to model physical systems. Simscape, SimDriveline, SimHydraulics, SimMechanics SimPowerSystems and extend the capabilities of modeling of physical systems containing mechanical, electrical and plumbing. Incorporating MATLAB code, you can call MATLAB functions for the analysis and visualization of data. Simulink also allows you to use the Embedded MATLAB code to create algorithms for distribution through integrated code generation along with the rest of the model. In addition, you can embed code C, Fortran, Ada and hand-written directly in the model, in order to create internal custom blocks. The models are created by dragging blocks from the library of belonging and dropping them in the graphical editor and connecting lines that establish mathematical relationships between them.

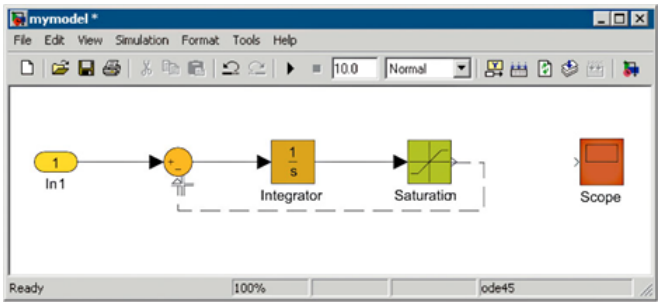

Figure 22: Options for connecting the blocks in Simulink. The blocks can be linked manually with the aid of the mouse or automatically by means of lines that represent the path between the blocks and through complex topologies

The user interface provides full control over what you can see and use on the screen. You can add commands and context menus and sub menus to the editor, as well as disable and hide menus, menu commands or controls in dialog boxes.

2.1.2 *Model organization*

Simulink allows you to organize your model into different hierarchical levels, thanks to the sub-systems and the technique of referencing the model (model referencing). The subsystems contain a group of blocks and the signals in a single block. You can

add a custom user interface to a subsystem hiding the content and presenting the subsystem as an atomic block, with a unique icon and a dialog specification of the parameters.

In addition, the model can be divided into various components for modeling, simulation and test each of them independently. The components can be saved as separate models using the referencing model or as subsystems in a library, and these are compatible with the systems configuration management, as well as with any application to control the recorded versions for Windows platforms.

You can reuse the components of the current project in other projects without problems and maintain the historical audit and review.

The organization of the models with this method allows you to specify the level of detail appropriate to the task at hand. In this sense, it is possible for example to use simple relationships for specific high-level modeling and add more detailed reports approaching the implementation phase.

The subsystems to allow conditional execution of altering the dynamics of the system by enabling or disabling specific sections of the project by means of signals of the control logic. Simulink allows to create the control signals to enable or trigger the execution of the subsystem at a particular time or in response to specific events.

With the logic blocks can be modeled simple commands to control the subsystems enabled. Stateflow allows to include a more complex control logic, as well as shaping machine states.

2.1.3 *Definition and management of signals and parameters*

Simulink allows you to define and control the attributes of the signals and parameters associated with the model: the signals are time-varying quantities represented by the lines connecting the blocks; the parameters are factors that help to define the dynamic behavior of the system.

The signal and parameter attributes can be specified directly in the diagram or in a separate data dictionary. With Model Explorer you can manage your data dictionaries and quickly alter a model incorporating different datasets. You can define the following signal and parameter attributes:

- Data type - integer single, double, signed or unsigned, 8, 16, or 32-bit fixed-point and boolean.
- Quote - scalar, vector, matrix or array nD.
- Complexity - real or complex values.
- Range minimum and maximum initial value and engineering units.

The types of fixed-point data provide support for scaling and arbitrary words in length up to 128 bits. These data types require the Simulink Fixed Point software to simulate and generate code.

You can also specify the sampling mode signal as a sample-based or frame, in order to run applications faster signal processing in Simulink and Signal Processing Blockset.

You can define data types and custom bus signals using the Simulink Data Objects. Bus signals are used to define the interfaces between the components of the project.

Simulink allows you to determine the level of specific signal, and if you do not specify the data attributes, Simulink determines them automatically by propagating. You can either specify only the interfaces of the component, whether all the data of the model: in each case, however, the consistency check is performed to verify the integrity of data.

You can limit the scope of the parameters to specific parts of the model, using a hierarchy of work spaces or sharing them between models through a common workspace.

2.2 MODELIZATION DEVELOPMENT STRATEGIES (MDS)

For the calibration generation, an internal CRF FPT tool has been developed, for the automatic generation of calibration tables from the experimental data acquired in field, the name of this tool is: Modelization Development Strategies (MDS) created by Fabio GUSTINETTI. [13]

The tool was entirely developed in Matlab according to the requirements of the control strategies development team for MultiAir applications. The computational software used in the thesis was Modelization Development Strategies (MDS). The MDS

tool was developed entirely in Matlab (rel 2006b) compared to the formulation of requirements made by the inspection team for the development of strategies for implementing Multiair. The tool manages MDS simulink models developed according to the rules agreed between Fiat Powertrain Technologies and Magneti Marelli, the methodology shared between the two companies in February 2006, requires the use of a shared library, a style common modeling and structured organization information associated with the strategies developed in co-design.

The development tools MDS aims to achieve the following goals:

1. Create a unique environment to support the developer's control strategies in matlab simulink.
2. Reduction of development of control strategies by 50%.
3. Splitting of the phases of the development process of the control strategies in sections of the tool.
4. Construction of sections of the tool inherently simple (limited number of services made available to the user).
5. Check real-time modeling of rules shared by Fiat Powertrain Technologies and Magneti Marelli.

The tool MDS appears to be composed of the following sections:

- MdlTemplate Creating Template simulation.
- CalAnalyzer Syntactic Analyzer Data Structure.
- Acquisition Manager test vectors for files of acquisition.
- Calibration Manager parameters calibrated to the calibration files.
- Simulation Environment Simulation of control strategies.
- TLReader Interpreter in reading the data entered on Target Link simulink model.
- Documentation Manager creating documentation in Word and PDF format.
- DataBase Database Data Structure.
- Merge Models Manager aggregate of strategies.

2.2.1 *MDS vs. process development strategies*

Are represented below the various phases of the development process of the control strategies and the use of the sections that constitute the tool MDS.

Step 1.

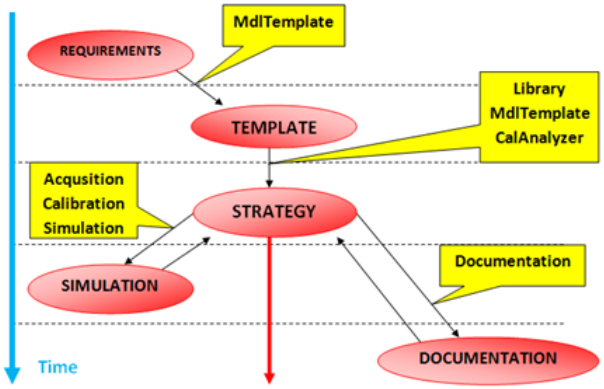

Figure 23: From the definition of the requirements to release control project under configuration tool

Step 2.

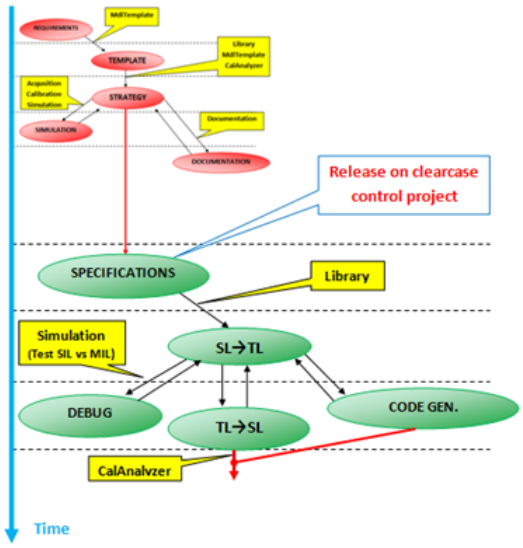

Figure 24: From the generation of C code to the release of the software project under configuration tool

Step 3.

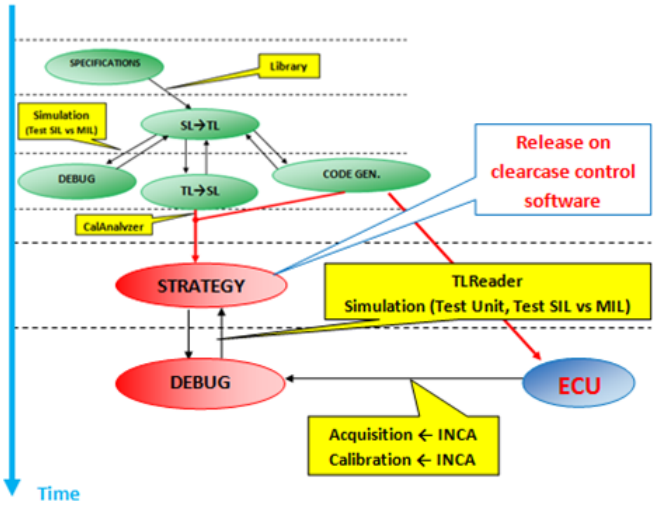

Figure 25: From TESTS software unit to unit testing of the control strategy

2.2.2 *Functional architecture of MDS*

The MDS tool is an instrument to support the developer of the control strategies during synthesis and modeling of the same algorithm in Matlab Simulink. The modeling of the control algorithm requires the creation of a well-defined set of files to support the Simulink model representing together with the latter the architecture of the so-called control project:

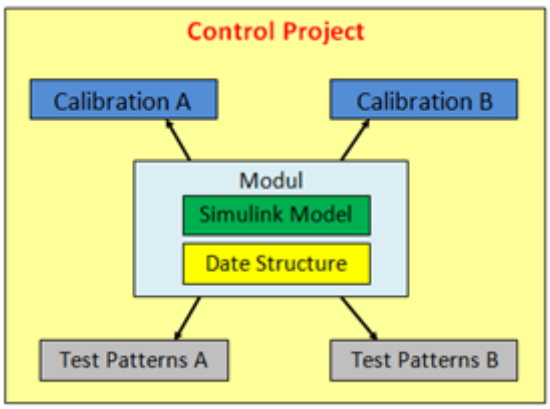

Figure 26: Control Project

The whole simulink model and data structure is placed at the 'center' of the project control project; they speak of methodology

module in the center. The files to support the strategy simulation derived from the module in terms of the consistency of content and alignment, the consistency of the content is checked on the basis of the information residing in the data structure namemodel_cal.m of the simulink model namemodel:

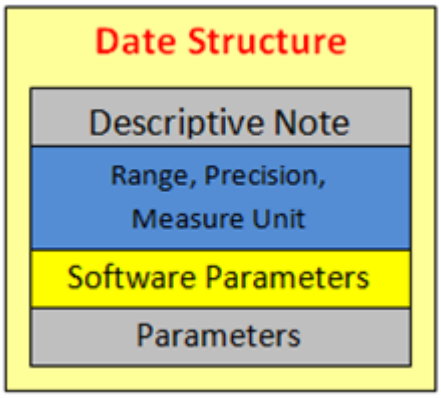

Figure 27: Data Structure

The sections of MDS were created mainly in order to provide the following services:

- Methods of assessment of Modeling Rules shared between Fiat Powertrain Technologies and Magneti Marelli.
- Automatic procedures for the streamlining of certain phases of the process of definition of control strategies.

Have been developed, in this sense, functions that have as objective to carry out the services listed and that are placed by an implementation point of view of MDS in distinct layers, each section appears to be organized in the following way:

If the verification fails Modeling Rules (diagnosis), is not made available to the user any kind of automatic procedure (control) but are notified of the type of anomaly and a description of possible solutions to be adopted.

The sections of MDS are related to each other, some of them are typically used in advanced stages of the development process of strategies:

In general, the use of these sections is independent from verification of the diagnostic functions of the sections used in the initial

part of the process of development of the models, according to the principles laid down by the methodology module to the center.

In the following examples are shown these relations:

2.2.2.1 *MdlTemplate*

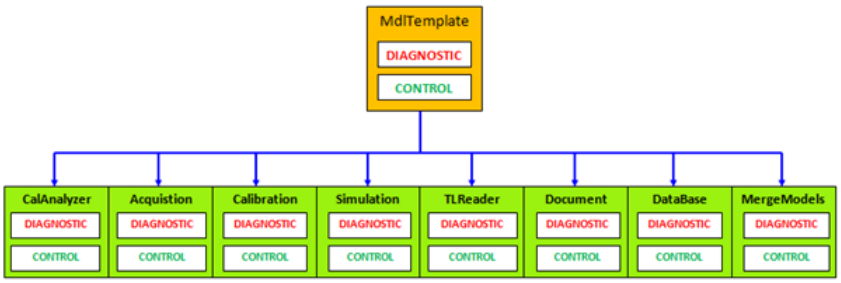

Figure 28: MdlTemplate vs MDS

The "MdlTemplate" aims to achieve the following objectives:

- Building a simulation environment to test the operation of a general strategy;
- Provide a data set of functions that allow the application of a general property of all the blocks used to synthesize the strategy;
- Driving you in learning the rules of architecture which must be synthesized with a control algorithm aimed at production code and correcting anomalies in each case providing directions on how to remedy;
- Provide a 'green dot' consistency about the architecture of the template simulation in order to ensure the application of the capabilities of MDS in the remaining sections.

2.2.2.2 *CalAnalyzer*

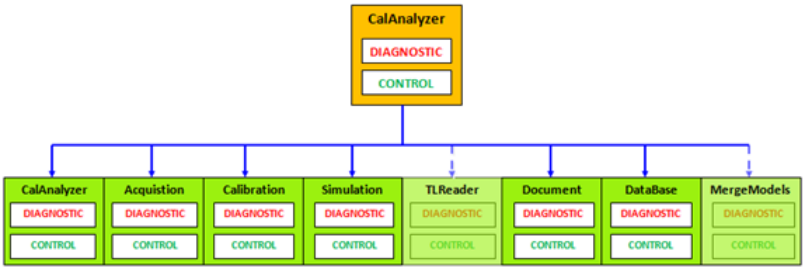

Figure 29: CalAnalyzer vs MDS

The "CalAnalyzer" aims to achieve the following objectives:

- Managing completely maintenance of data structures associated with the simulink models by providing a 'green dot' data consistency;
- Apply during the development of strategies modeling the rules shared by Fiat Powertrain Technologies and Magneti Marelli, verifying the user's request the syntactic and semantic correctness of the new structured data input;
- Ensure alignment between structure and data model;
- Drive the user in learning the rules for the compilation of the data structure and in the correction of anomalies in each case providing directions on how to remedy;
- Create a graphical environment-oriented navigation of the data structure in order to improve consultation of all its content.

2.2.2.3 *Acquisition*

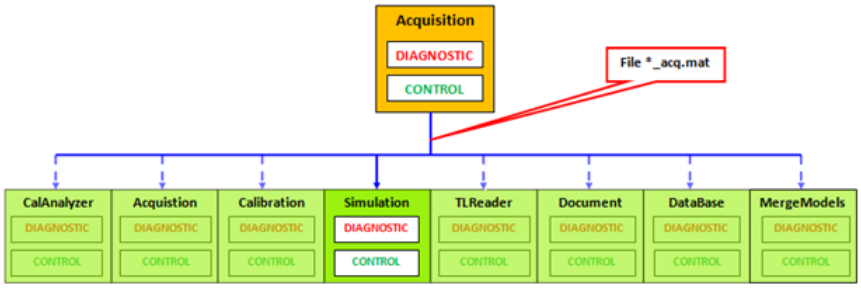

Figure 30: Acquisition vs MDS

The "Acquisition" aims to achieve the following objectives:

- Manage the maintenance and creation of fully test vectors used for the simulation and verification of control strategies by providing a 'green dot' data consistency;
- Apply during the development of test vectors modeling the rules shared by Fiat Powertrain Technologies and Magneti Marelli, verifying the correctness of the user request profiles placed in relation to the definition of the variables in the interface data structure;
- Ensure a link between the acquisition of control from development tools and INCA test vectors to be used on simulink model;
- Driving you in learning the rules of maintenance of test vectors and correcting any anomalies providing case by case basis directions on how to remedy;
- Create an environment oriented graphic display and modification of test vectors;

2.2.2.4 *Calibration*

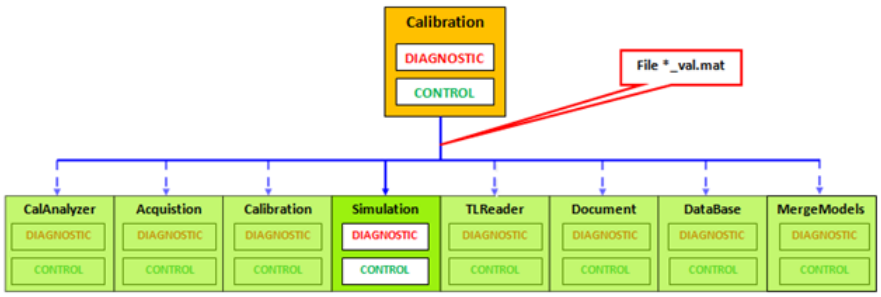

Figure 31: Calibration vs MDS

The section "Calibration" aims to achieve the following objectives:

- Manage the maintenance and creation of fully calibrated parameters used for the simulation and verification of control strategies by providing a 'green dot' data consistency;

- Apply during maintenance of the parameters calibrated the modeling rules shared by Fiat Powertrain Technologies and Magneti Marelli, verifying the user's request the correctness of the values entered in relation to the definition of the relevant structured objects in the data structure;
- Ensure a link between calibrations of control from development tool INCA and the parameters calibrated for use on simulink model;
- Driving you in learning the rules of maintenance of the calibrated parameters and correcting any anomalies present case by case providing guidance on how to remedy;
- Create an environment oriented graphic display of the parameters calibrated;
- Export format compatible INCA calibrated parameter values used by a generic strategy.

2.2.2.5 *DataBase*

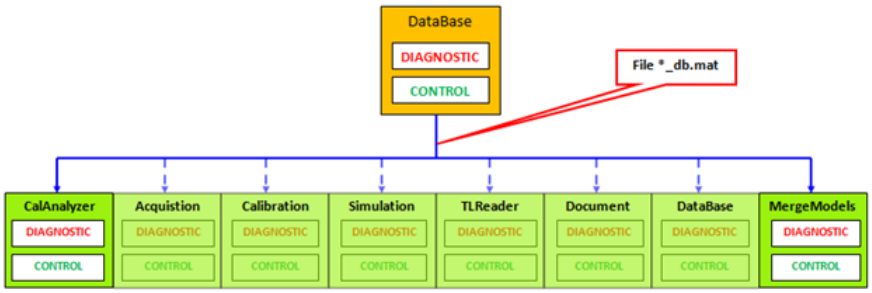

Figure 32: DataBase vs MDS

The "Database" aims to achieve the following objectives:

- Creation of a database of structured objects for the application from simulink models 'Modeling Rules' compatible (bottom-up approach);
- Creation of a graphical environment for the visualization of structured objects in the database
- Generate excel document to BOM (simulink models);

- Generate files for the integration of extension _db.mat to be made available to the sections:

"CalAnalyzer" →Top-Down Approach for updating the data structure

"Merge" →Generation aggregates strategies

2.2.2.6 *MergeModels*

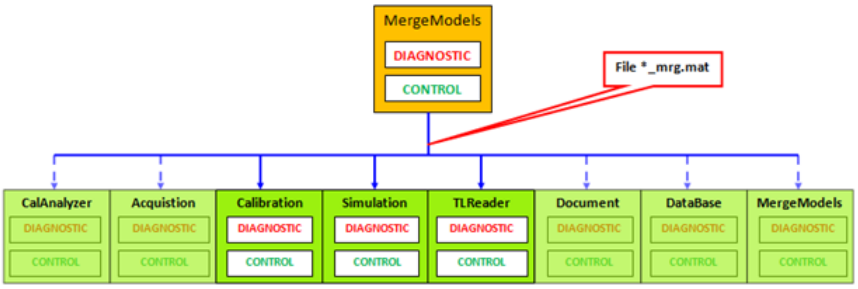

Figure 33: MergeModels vs MDS

The "MergeModels" aims to achieve the following objectives:

- Creation of an aggregate of strategies from simulink models 'Modeling Rules' compatible (bottom-up approach);
- Creation of a graphical environment for the visualization of structured objects contained in the aggregate of strategies;
- Management module interfaces, functional sub-areas, functional areas aggregates of strategies.
- Generation for the areas, subareas, and aggregates of strategies:
  - Data Structure.
  - Stubs software.
  - Tables PDF.
  - Implementation specifications of Operation (Word).

- Storage of aggregates strategies and creating an export file extension * _mrg.mat to be used in the sections:
  - Acquisition.
  - Calibration.
  - Simulation.

2.2.2.7 *Simulation*

The "Simulation" aims to achieve the following objectives:

- Manage a system of integrated plot-oriented simulation of the control strategy (15 plots of 16 variables each);
- Generate a report simulation;
- Perform unit testing of control strategies;
- Generate a report of unit testing;
- Compare 2 simulations using the same parameter file calibrated and 2 discrete files with the test vectors;
- Load and display acquisitions exported from INCA and test tracks from TargetLink (Modeling and Software In the Loop In the Loop).

2.2.2.8 *TLReader*

The "TLReader" is proposed as the only goal of reading the information "Link Target" store owners of the fields (field tag) simulink blocks: the display in simulink environment of such information enables you to develop with greater awareness of control strategies aimed the generation of a production code.

2.2.2.9 *Documentation*

The section "Documentation" aims to achieve the following objectives:

- Provide a 'green dot' data consistency as to allow the insertion of the documentation simulink model;
- Manage the entry and maintenance of documentation in the simulink model;
- Create an environment oriented graphic display of the documentation included with the simulink model;
- Create documentation files in Word format (Specify realization of Operation) and PDF (Tables Strategy) from the information included in the simulink model and the data structure.

Part II

THE MODEL

In the control chain for management the Low Pressure EGR system, unique computational modules are defined to carrying out a specific task. Each module is created using Simulink, is verified through MDS and then is inserted into the ECU which will be connected to the corresponding sensors.

The second part of the thesis consist in the model under study, explaining each of its parts and what improvements or modifications have been done. Also have been developed in detail each of the new parts will be included and finally is described the verification process.

3

CEGR MODEL

One of the module responsible for the LP EGR throttle management is the CEGR model, is in charge to control the EGR mass flow through the LP EGR system and the delay associated to the duration of the travel of the mass until arrive to the EGR throttle valve.

3.1 CEGR OPERATIONAL GOALS

The goal of CEGR module is to define the upstream pressure target through the management of the EGR throttle valve, this is linked with the following objectives:

- Regulation of the amount of EGR mass flow that will be introduced into the manifold, defining the correct angle;
- Establish the limits (maximum and minimum) for avoid damage in the EGR throttle valve;
- Define the delay associate to the travel adequate for each situation.

3.1.1 *Global overview*

The global overview of the CEGR module (Figure (34)) contains 3 main blocks:

1. CEGR_Scheduler
2. CEGR_Setup_Call
3. CEGR_Main_Calc

Between of them only the green block is studied, considering that the gray ones are system blocks that do not require a modification. At the same time, the color description for the different variables are the following:

- *Blue*: new variables that are introduced into the module (PEXHO2SENS, PINCOMP and TOUTTWC).
- *Orange*: variable that is previously present in the module but will be used in the new part (QEGRH).
- *Yellow*: variables that are used in the other methods to obtain the EGR throttle valve angle (ETAEGRMAX, QAH, RPM, ETASOBJ and TH2OC).
- *Red*: output variables, in the Fig. (34) is the EGR throttle valve angle (ANGFAR_EGRLP).

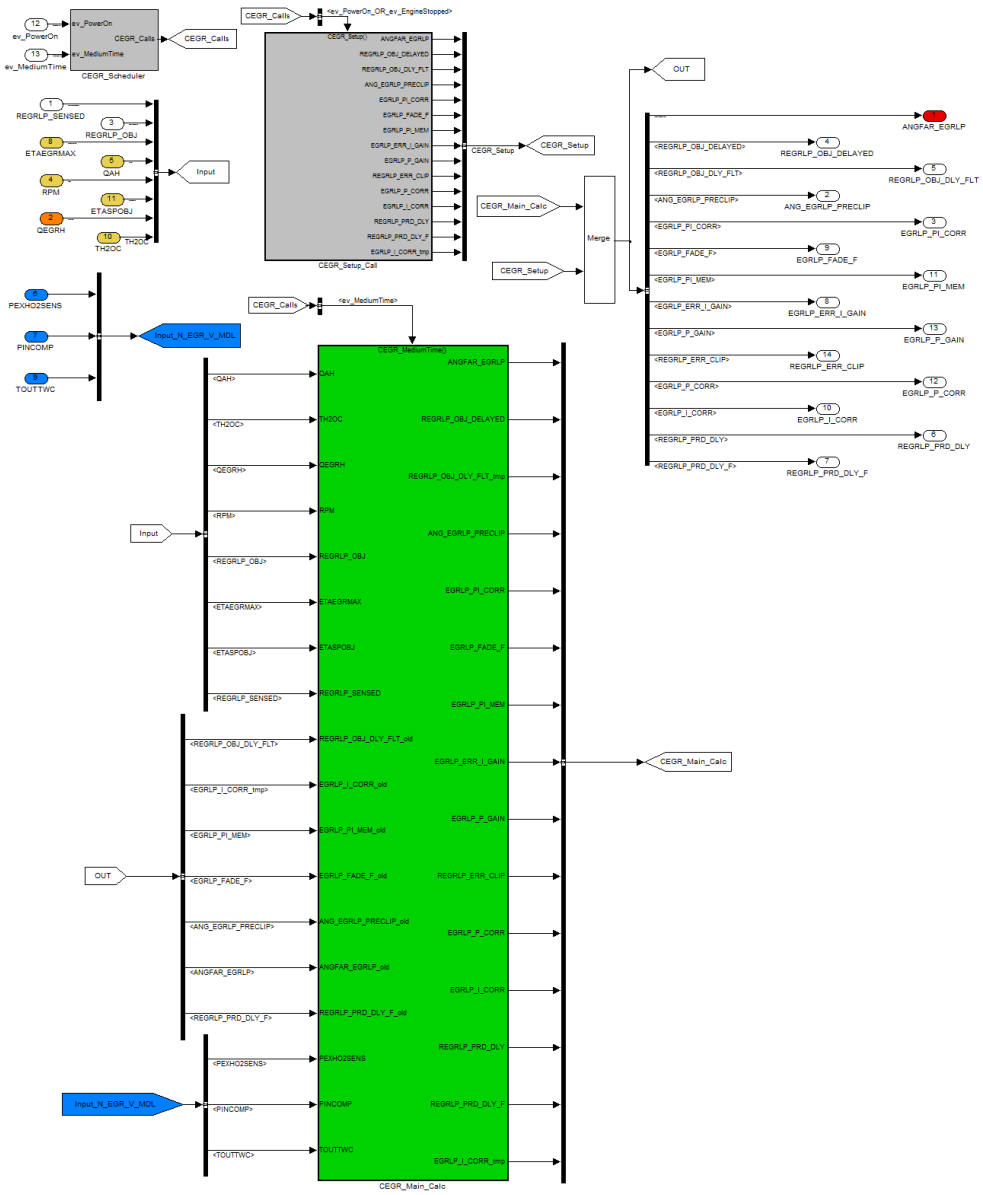

Figure 34: CEGR module - Global overview

3.1.1.1 *CEGR_Main_Calc block*

The main calculation block of the CEGR module (Figure (35)) as the name says, is responsible for performing the main calculations during the following events or conditions:

- ev_PowerOn: Power On event (is when the switch is passed without start the cranking phase).
- ev_MediumTime: Medium Time event (occurs every 12 ms, the different sensors are regulated each time interval).

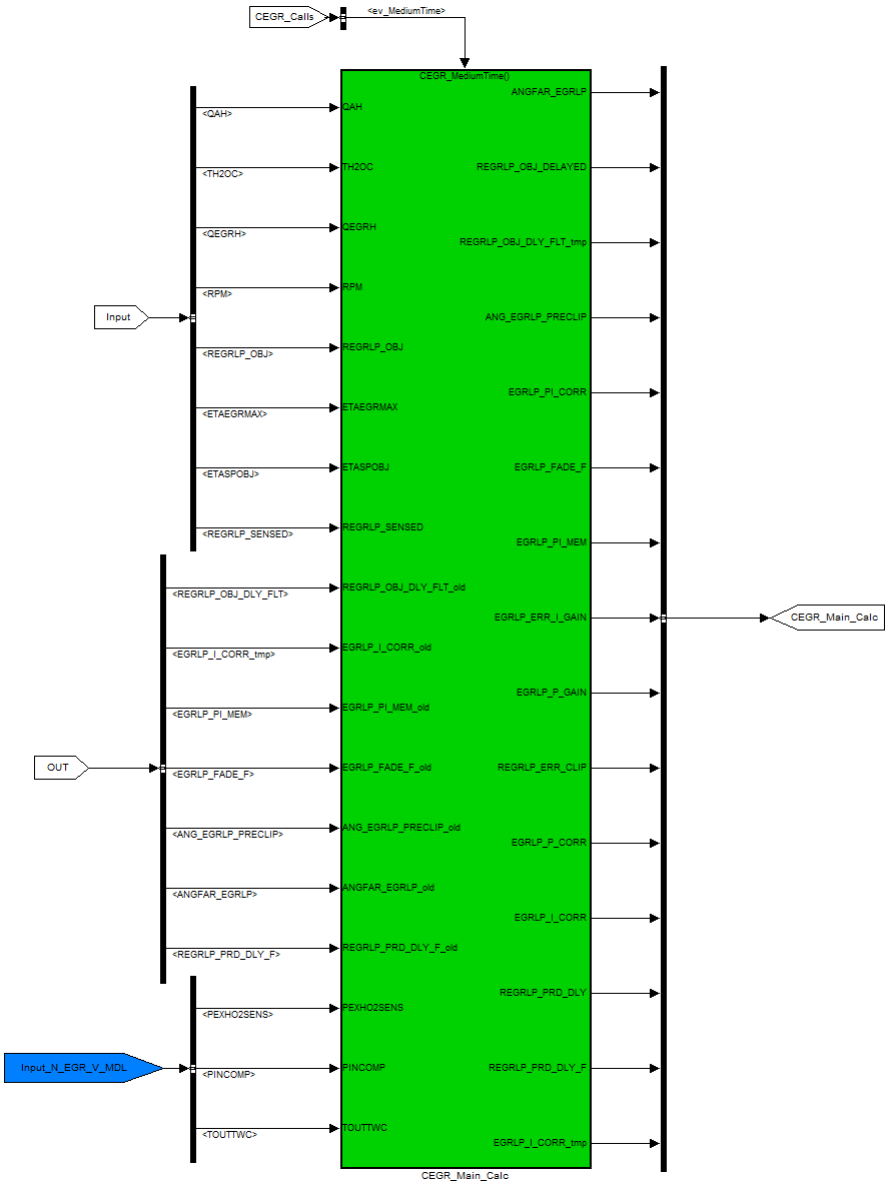

Figure 35: CEGR__Main__Calc interface

Moreover, in the Fig. (36) it is possible appreciate in color light blue the path to be followed to perform the calculation of the EGR throttle valve angle without delay and specifically using the new model inserted. Also, the two blocks in yellow are the methods already available to calculate the EGR throttle valve angle, which will be explained in details later.

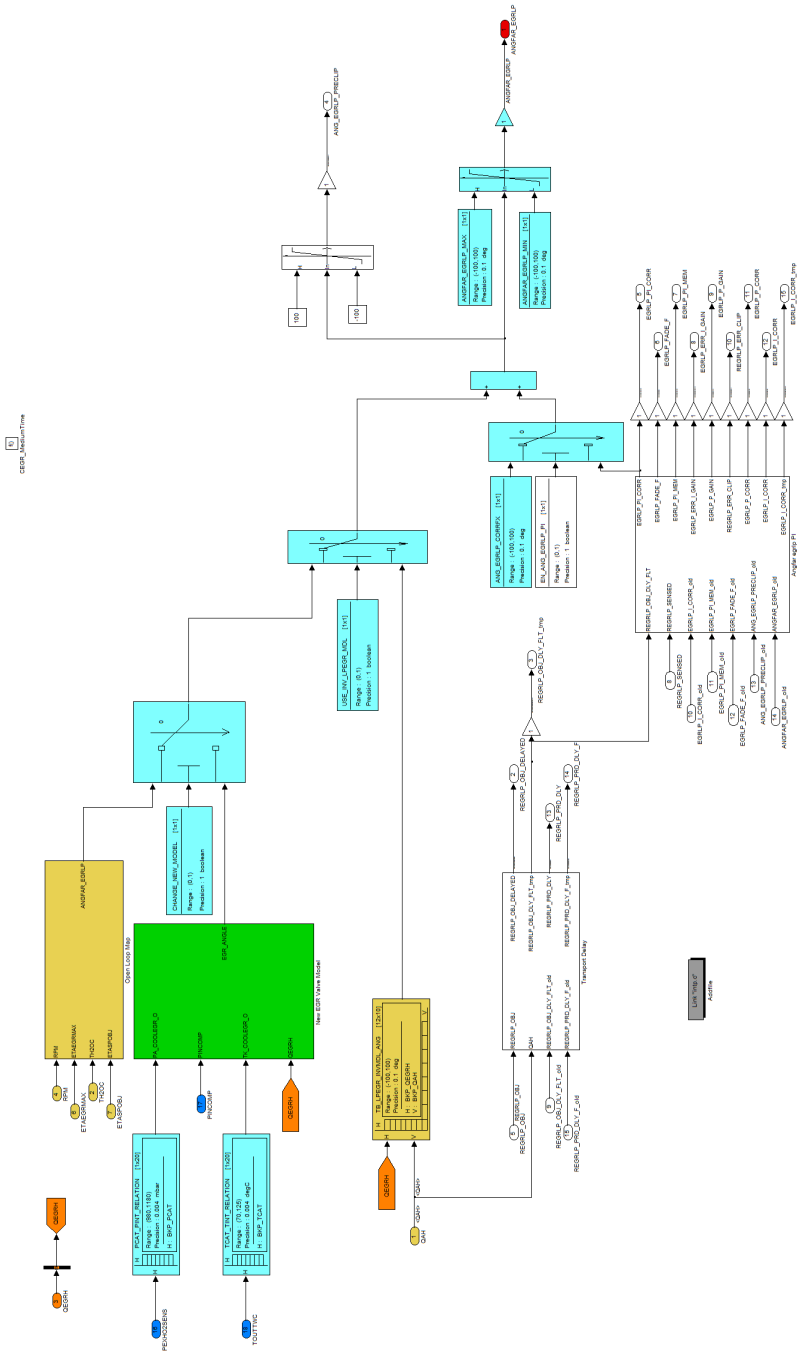

Figure 36: Inside CEGR_Main_Calc

3.2 EGR THROTTLE VALVE ANGLE CALCULATION

Actually inside of the module two different sections exist that perform the calculation of the EGR throttle valve angle. The first, is a map (called “Table LP EGR inverse model angle”) and the second

is a block (called “Open Loop Map”) composed by several maps and operations. Initially the two methods working without the corresponding delay to the transport the EGR mass flow, which is added in the final part as a contribution to the angle, where may be fixed or calculated.

Due to the difficulties to obtain a correct relation between the quantity of EGR mass flow and the angle of the EGR throttle valve angle, it is necessary to propose an alternative to the current techniques that calculate this relation, with the principal aim of obtaining greater accuracy in the quantity of EGR that is needed and the quantity that effectively enters into the manifold.

Below in the Fig. (37) are the two basic schemes of the methods responsible for determine the EGR mass flow/EGR throttle valve angle relation and the new model proposed:

- Table LP EGR inverse model angle (TB_LPEGR_INVMDL_ANG):
- Open loop map.
- New model EGR valve.

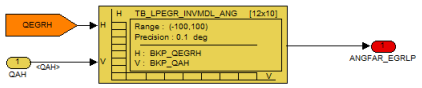

(a) Table LP EGR inverse model angle

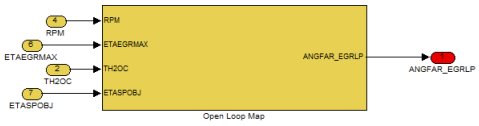

(b) Open Loop Map

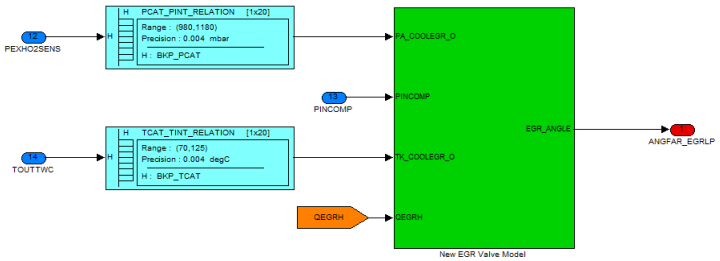

(c) New model EGR valve

Figure 37: Basic Schemes of the methods responsible for determining the EGR mass flow/Valve angle relation

3.2.1 *Table LP EGR inverse model angle*

3.2.1.1 *General overview*

The table LP EGR inverse model angle is a map that takes into consideration the quantity of fresh air $[kg/h]$ and EGR mass flow $[kg/h]$ to calculate the EGR throttle valve angle. This table is a simple relationship between the two aforementioned parameters and the EGR throttle valve angle without any theoretical basis, the calculation is performed through simulink program.

In the Fig. (38), is shown the schematic representation in the software:

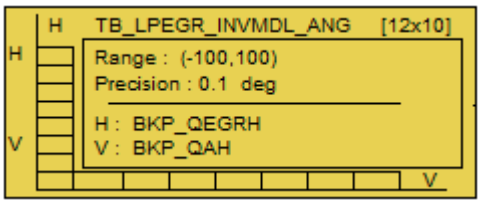

Figure 38: General overview - TB_LPEGR_INVMDL_ANG

3.2.1.2 *Inputs and output description*

The variables that are used to determine the EGR throttle valve angle in this case are:

- QAH: air intake capacity per hour for all cylinders, is provided by the IASP module.
- QEGRH: EGR intake capacity per hour for all cylinders, is provided by the CQLC module.

The output obtained is:

- ANGFAR_EGRLP: EGR throttle valve angle.

3.2.1.3 *Units table*

VARIABLE	UNIT
QAH	[kg/h]
QEGRH	[kg/h]
ANGFAR_EGRLP	[°]

Table 1: Units table - TB_LPEGR_INVMDL_ANG.

3.2.2 *Open loop map*

3.2.2.1 *General overview*

In this open loop map the EGR throttle valve angle is determined through the target intake efficiency (related to the required load / volumetric efficiency) and a relation with the engine speed (RPM). The aim is achieve through a map (correctly calibrated) the valve angle using the target intake efficiency.

In other models with the load required (related with the target intake efficiency) and engine speed was possible obtain the required EGR mass flow, then are looking a similar relationship with the angle, considering the water temperature correction and the limitations for the maximum and minimum value of EGR mass flow that the engine can aspirate.

Below, is shown the general schedule of the proposed map.

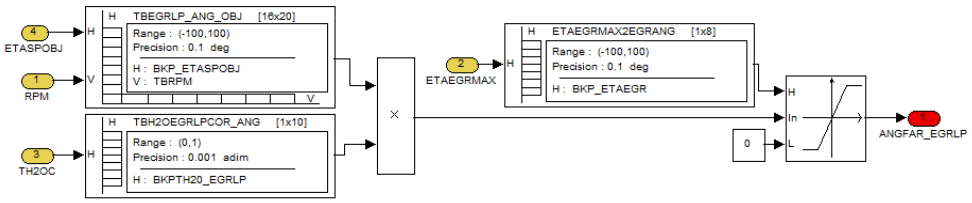

Figure 39: General overview - Open loop map

3.2.2.2 *Inputs and output description*

For this model, the inputs are listed as follows:

- ETASPOBJ: target intake efficiency. Represents the total mass flow of air (fresh air and EGR mass flow) that is introduced for a specific combustion cycle.
- RPM: engine speed.
- TH2OC: is the correct water temperature. This is the water temperature in the radiator and is taken into account to avoid the use of EGR during the condition at which the temperatures are lower a certain limit and therefore the EGR could affect the stability of the combustion process.
- ETAEGRMAX: maximum normalized estimated external EGR mass flow that the engine can aspirate.

The output obtained is:

- ANGFAR_EGRLP: EGR throttle valve angle.

3.2.2.3 *Units table*

VARIABLE	UNIT
ETASPOBJ	[adim]
RPM	[rpm]
TH2OC	[°C]
ETAEGRMAX	[adim]
ANGFAR_EGRLP	[°]

Table 2: Units table - Open loop map.

3.2.3 *New model EGR valve*

3.2.3.1 *General overview*

This is the new model that will be developed, here is considered the input and output pressures, input temperature and the EGR mass flow that is requested to pass through the EGR throttle valve; it is important to know that these inputs are not available in a real engine and only in a test bench engine, which generates a higher difficulty to get a good estimate for the required valve angle, but using maps to estimate these inputs is possible, getting a more practical result

The general overview is shown in the Fig. (40).

3.2.3.2 *Inputs and output description*

In the new model the inputs that will be considered are:

- PEXHO2SENS: output pressure of the catalyst (shown in the Fig. 37c).
- TOUTTWC: output temperature of the catalyst (shown in the Fig. 37c).
- PINCOMP: input compressor pressure.
- QEGRH: amount of EGR mass flow required.

The output obtained is:

- EGR_ANGLE: EGR throttle valve angle.

3.2.3.3 *Units table*

VARIABLE	UNIT
PEXHO2SENS	[mbar]
TOUTWC	[°C]
PINCOMP	[mbar]
QEGRH	[kg/h]
EGR_ANGLE	[°]

Table 3: Units table - New model EGR valve.

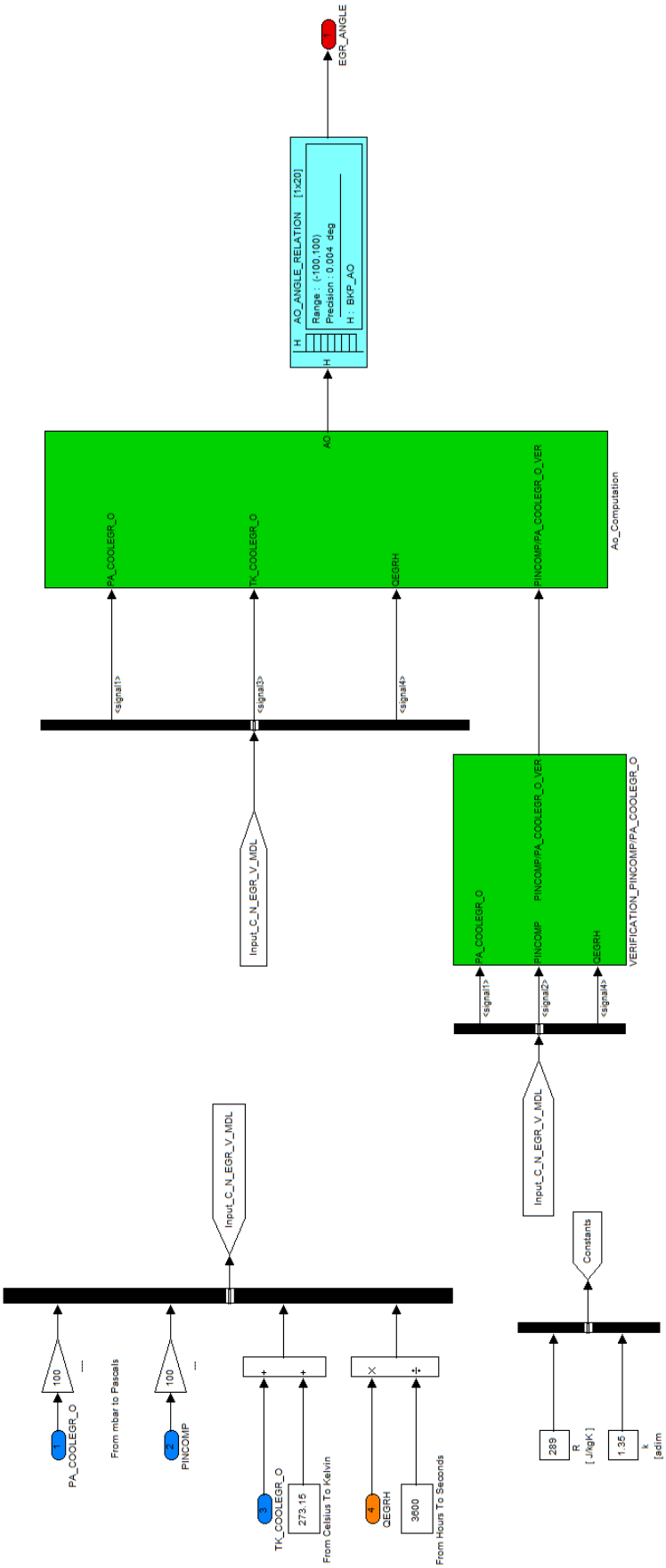

Figure 40: General overview - New model EGR valve

4

NEW EGR VALVE MODEL

In this chapter the process to develop the New EGR Valve Model will be described. The order to explain the new model is the following:

1. Theoretical basis that was used to perform the model.
2. Explanation for obtaining the necessary input parameters that allow to calculate the EGR throttle valve angle.
3. The different parts that make up the model.
4. Boundaries that are introduced to avoid a not physically consistent results.
5. Verification process to validated the model through the engine experimental data. [14]

4.1 THEORETICAL BASIS TO DEVELOP THE MODEL

As was found in the previous chapter, the objective of this new model is obtain through the available data in a series production engine, the valve angle to effectively regulate the amount of exhaust gases that are required in a specific condition.

For this, it provides a database that will allow to create the model and also make the verification .

Meanwhile, with regard to the theoretical basis, the mass flow-rate through the EGR control-valve is described by the Compressible-Flow Nozzle equation [15]. This equation is derived from a quasi-steady one-dimensional flow analysis and the real effects are included in the model by means of an experimental discharge coefficient.

The equation below describe the flow of a gas from a plenum at state 0 (inlet of the throttle valve), through a short tube, to a pressure $Pout$ downstream of the tube [16]:

$$\dot{m}_{EGR} = A_o \frac{P_{in}}{\sqrt{RT_{in}}} \sqrt{2\frac{k}{k-1}\left[\left(\frac{P_{out}}{P_{in}}\right)^{\frac{2}{k}} - \left(\frac{P_{out}}{P_{in}}\right)^{\frac{k+1}{k}}\right]} \quad (7)$$

Where:

- $\dot{m}_{EGR}$ = EGR mass flow.
- A_o = parameter that contain the discharge coefficient and the throttle plate open area.
- R = is the elastic constant of the exhaust gases (also called individual gas constant). A constant value of R was selected, regardless of the considered engine working condition. The variation in the average molecular weight of the exhaust gases with their composition was verified to be within 1% and its effect on R was therefore neglected.
- k = heat capacity ratio [1]. Is the value of the polytrophic evolution law exponent for the cooled flow (as already mentioned, the EGR control-valve is cooled).
- P_{out} = output pressure of the convergent nozzle (assumed equal to the pressure at the inlet of the compressor):
- P_{in} = is the pressure upstream of the EGR cooler (assumed equal to the pressure at the restricted flow-area of the control valve).
- T_{in} = input temperature of the convergent nozzle

The Equation 4.1 is handly if stagnation conditions are known and the velocity is not choked [2]; and in the new model the velocity of the flow never reach the choked condition [17] (also called critical condition), where the pressure relation (P_{out}/P_{in}) in all the cases is higher than 0.528 and lower than 1, that allow to work with the equation previously presented (graphically represented in the Figure (41)); existing only a little difference after and before the EGR throttle valve.

1 Is the ratio of the heat capacity at constant pressure (Cp) to heat capacity at constant volume (Cv).

2 Choked flow is a limiting condition which occurs when the mass flow rate will not increase with a further decrease in the downstream pressure environment while upstream pressure is fixed.

Using the equation above, is possible to create a chart that relates the A_o variable with the angle of the EGR throttle valve.

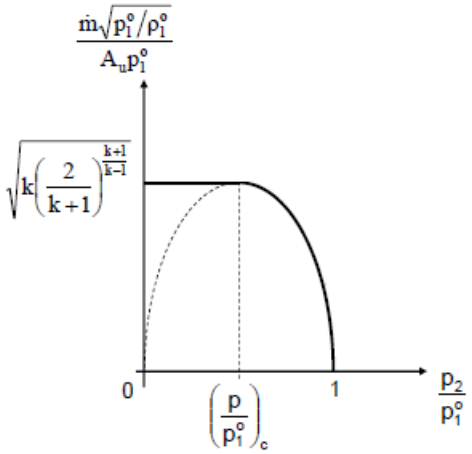

Figure 41: Schematic representation of the Compressible-Flow Nozzle equation

4.2 BUILD UP THE INPUT PARAMETERS

As explained in the previous chapter, the inputs for the new model are:

- PEXHO2SENS.
- TOUTWC.
- PINCOMP.
- QEGRH.

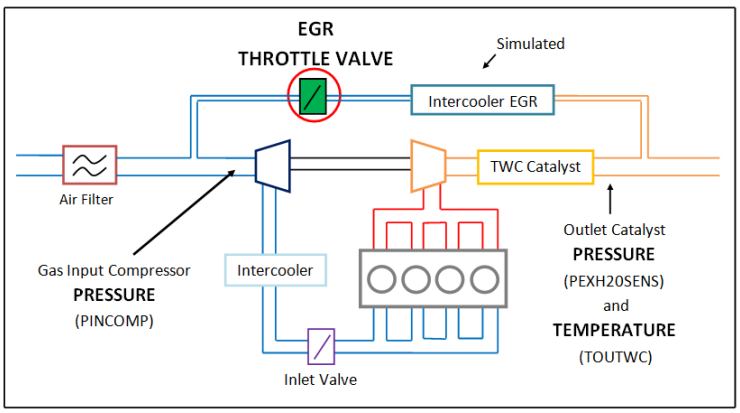

Figure 42: Schematic representation of the LP EGR system with the corresponding available data

In the Figure (42) is possible observe the Low Pressure EGR configuration, also are highlights the parameters available in the database. Is clear that the input temperature and pressure are not corresponding to the throttle valve inlet; instead are the temperature and pressure of the outlet of the catalyst, this happens because the production engine does not have the same quantity of sensors (i.e. measurements) that could be installed in a test bench engine due to the production cost.

The new EGR valve model attempts to reproduce the real conditions of an engine, therefore two maps were used to simulate the temperature and pressure valve inlet which are also outlet temperature and pressure of the intercooler, as shown in Fig. (42).

4.2.1 *General specifications of the engine used to construct the initial maps and the another parameters*

For obtain the different maps and parameters that allow to create the model was used a four cylinder gasoline engine with the following characteristics:

CHARACTERISTIC	VALUE	UNITS
Compression ratio	9.8	[adim]
Bore	72	[mm]
Stroke	84	[mm]
Connecting rod length	129	[mm]

Table 4: General specifications of the engine used to construct the maps

The experiments in the testbench were running in two phases:

- First, at 2250, 3000 and 4000 rpm, with these data was performed the maps for the inlet pressure and temperature of the EGR throttle valve. However, these data base was not used to build up the model due to imprecision and the results were not physically consistent during the recollection of the EGR mass flow data.

- Second, at 2500 rpm - 1500 mbar, 2500 rpm - 1900 mbar and 4000 rpm - 1500 mbar, with these data were performed the other maps to calculate the EGR throttle valve angle. Also,

all maps needed consider the three rpm mentioned thus cover higher range.

It is important to note that a sample was selected from the last database to build up each map. The data selection process was simple, every 100 data is selected a value for to be used on the maps, thus obtaining 571 values over a 57.100 data, these data are discarded during the verification process.

4.2.2 *Catalyst and intercooler temperature relation map*

To build the model of the outlet EGR intercooler absolute temperature will be used data from the engine that was previously mentioned; where having the input/output data of the intercooler and representing these two data in Excel is possible get a trendline. While it may obtain the equation that represents this line and will be used to create the map, i.e. introducing a certain catalyst outlet temperature could be estimated the outlet temperature of the intercooler.

Presented in the figure below are graphed these two data with the corresponding trendline and its equation.

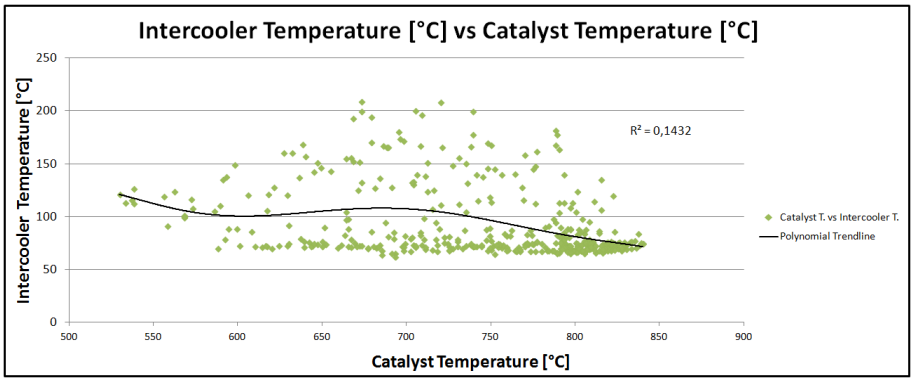

Figure 43: Catalyst and intercooler temperatures relation map - Chart and trendline.

$$\begin{aligned} T.Intercooler = {} & 3,47E^{-11}(T.Catalyst)^6 - 1,34E^{-07}(T.Catalyst)^5 \\ & + 2,16E^{-04}(T.Catalyst)^4 - 1,85E^{-01}(T.Catalyst)^3 \\ & + 8,87E^{+01}(T.Catalyst)^2 - 2,26E + 04(T.Catalyst)^1 \\ & + 2,39E^{+06} \end{aligned} \quad (8)$$

One can see that the trendline obtained is not very accurate and does not reflect actual behavior of the data. For this reason, it is possible that the temperatures within the intercooler being affected by an additional parameter that is not considered in this study. Theoretical and experimental results showed that thermal effectiveness in the intercooler mainly depended on: the EGR mass flow-rate, the thickness of the fouling layer, the temperature of the hot gas and also the mass flow-rate of the coolant. [18]

Can be done a future study, to develop an in-depth analysis to see what happens inside the intercooler, thus generating a much more accurate estimate and see if it can add another parameter to obtain greater accuracy.

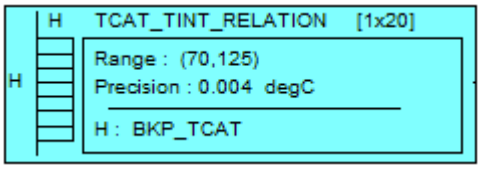

Figure 44: Simulink representation of the catalyst and intercooler temperatures relation map

In the Figure (44) can be seen that this map in the new EGR valve model is called TCAT_TINT_RELATION, which enter the catalyst outlet temperature and this will provide the intercooler outlet temperature, that inside in the new EGR valve model is called TK_COOLER_O[3].

4.2.3 *Catalyst and intercooler pressures relation map*

As in the previous map, the graph is constructed through data from the respective engine, is obtained the chart, trendline and the equation.

3 TK_COOLER_O: Outlet intercooler exhaust gas recirculation temperature.

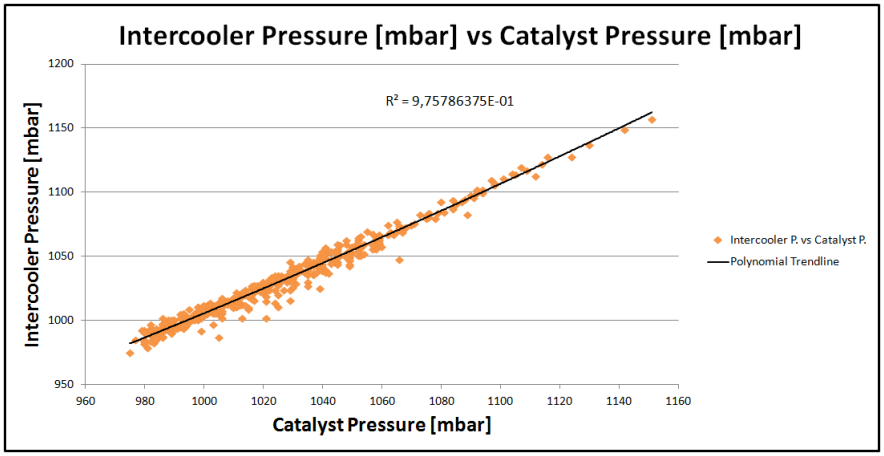

Figure 45: Catalyst and intercooler pressures relation map - Chart and trendline

$$\begin{aligned} P.Intercooler = {} & -2,13E^{-11}(P.Catalyst)^6 + 1,35E^{-07}(P.Catalyst)^5 \\ & - 3,55E^{-04}(P.Catalyst)^4 + 4,98E^{-01}(P.Catalyst)^3 \\ & - 3,93E^{+02}(P.Catalyst)^2 + 1,66E^{+05}(P.Catalyst)^1 \\ & - 2,90E^{+07} \end{aligned} \quad (9)$$

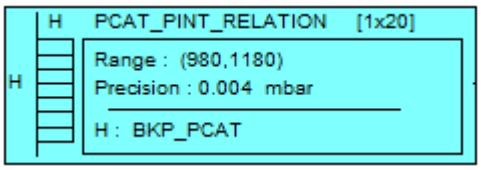

Figure 46: Simulink representation of the catalyst and intercooler pressures relation map

In this case as is seen in the Figure (46) the map is known as PCAT_PINT_RELATION and the outlet intercooler pressure in the new model will be called: PA_COOLEGR_O[4].

4.3 UNIT CONVERSION SECTION

Is represented below in the Figure (47) the different units conversion procedures for each data input and also presented in Table 5 the units before and after its conversion for a better compression.

4 PA_COOLEGR_O: Outlet intercooler exhaust gas recirculation pressure.

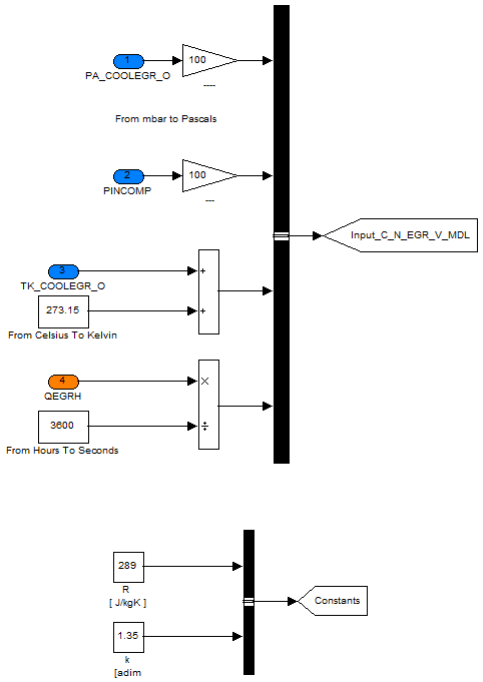

Figure 47: Simulink representation of the unit conversion section for the input data

PARAMETER	AFTER	BEFORE
Pressure	[mbar]	[Pa]
Temperature	[°C]	[°K]
Flow rate	[kg/h]	[kg/s]

Table 5: Inputs units before and after its conversion.

In the picture (Fig. 47) it can also be observed the values assigned to the constants in the Equation 7. These values are:

- $R = 289\ J/kg°K$.
- $k = 1.35$.

4.4 PINCOMP/PA__COOLEGR__O VERIFICATION BLOCK

Now, going to the verification block, is found the block that is responsible for removing all the possible values of the pressure relation who are above the maximum allowed, i.e. higher than 1, that are not physically consistent results. As shown in Figure

(48) the block is composed of two different checks (maximum and minimum), the entries are:

- PA_COOLEGR_O
- PINCOMP
- QEGRH

In this case the output parameter is PINCOMP/PA COOLER_O_VER that represent the pressure relation verified.

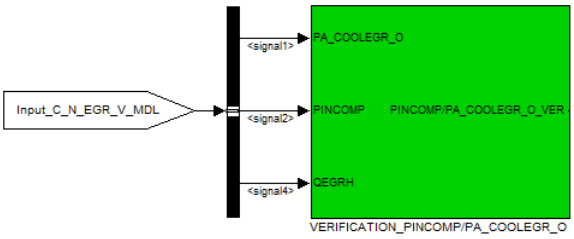

Figure 48: Verification PINCOMP/PA_COOLEGR_O block

4.4.1 *PINCOMP/PA_COOLEGR_O minimum verification block*

If the EGR mass flow required is lower or equal than the minimum value permitted (zero value of EGR mass flow), the system starts using the minimum verification block that is in the bottom part. In the contrary will be passed to the maximum verification block.

In the Figure (49), the first step is to compare the QEGRH mass flow with the minimum value that could be introduced into the system, logically is 0 kg/s (QEGRH_MIN), the possible pathways are:

1. If QEGRH $>$ QEGRH_MIN: the pressure ratio comes out without any modification in this part.
2. If QEGRH $\leq$ QEGRH_MIN: means that the EGR throttle valve should be completely closed (angle 8°, was explained in Section 1.5). For this reason the pressure relation is compared with a not physically consistent value[5] to verify that there are no mistake that could be obtained with 0 kg/s of EGR mass flow. The value considered not correct is one (1) because there will always be a difference pressure.

5 Gives an incorrect value because when introduced into the equation 7 is obtained a negative value inside the square root

To avoid infinite results in the calculation of the A_o parameter in the Section 4.1, the pressure relation is changed to a lower value, specifically to a value 0.01% lower than the number that generate error, which although changes the A_o results, not affect the final result because the model is limited in the extreme to avoid EGR throttle valve angle values below a certain number. The only function of this is to guaranty obtain a reliable value for pressure relation when the EGR mass flow is equal to 0 kg/s; the analysis that is behind of this verification was found during the model simulation.

Finally, the PINCOMP/PA_COOLEGR_O_VER_MIN is obtained and is the minimum verification for the pressure relation.

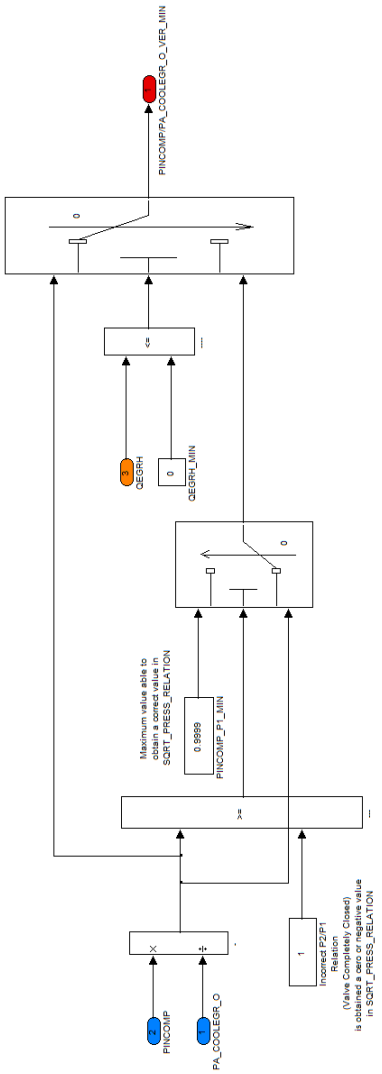

Figure 49: PINCOMP/PA_COOLEGR_O minimum verification block

4.4.2 *PINCOMP/PA_COOLEGR_O maximum verification block*

The case that here is evaluated is for a EGR mass flow equal or higher than the maximum allowable. During the simulation was observed that sometimes errors existed regarding pressure ratios greater than one with very large EGR masses flow. Therefore, was established as maximum value for the pressure relation 0.9919 that is the number obtained for the maximum EGR throttle valve angle (51.6607°) found from the experiment data.

The Figure (50) shows that the verification starts with the comparison of the pressure ratio with the maximum value (0.9919), and exhibits two possible paths:

1. If PINCOMP/PA_COOLEGR_O $\leq$ 0.9919: the pressure ratio comes out without any modification.
2. If PINCOMP/PA_COOLEGR_O >0.9919: the pressure ratio is changed for this value, to obtain the maximum EGR throttle EGR valve angle.

The output displayed is PINCOMP/PA_COOLEGR_O_VER_MAX that is the maximum verified value for the pressure relation.

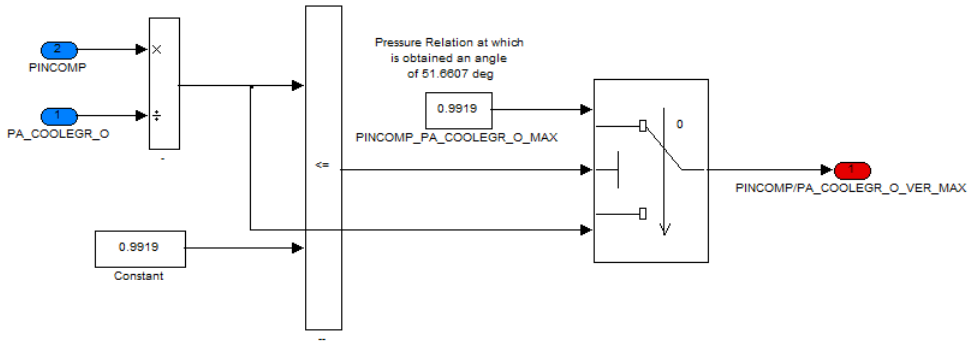

Figure 50: PINCOMP/PA_COOLEGR_O maximum verification block

4.5 AO_COMPUTATION

The following step consisted in translating the Equation 4.1 into a Simulink format, in the Figure (51) it is possible to observe the inputs and output from the Ao_Computation block, and the corresponding variables are:

- Inputs
  - $\dot{m}$: QEGRH_VER
  - R: R
  - k: k
  - P_{out}/P_{in}: PINCOMP/PA_COOLEGR_O_VER
  - T_{in}: TK_COOLEGR_O
- Output
  - A_o: AO

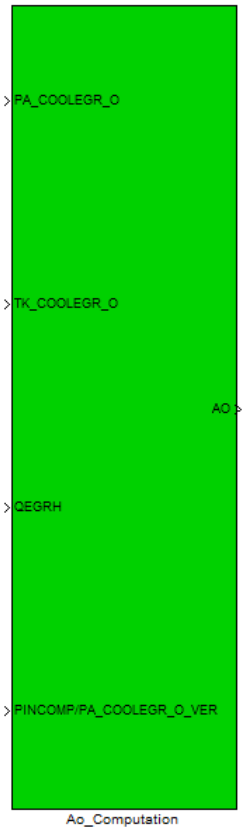

Figure 51: Ao_Computation

At the same time, in the Figure (52) is shown the internal view of the Ao_Computation block. At the left side (Table 6), the block starts with the calculation of two different maps:

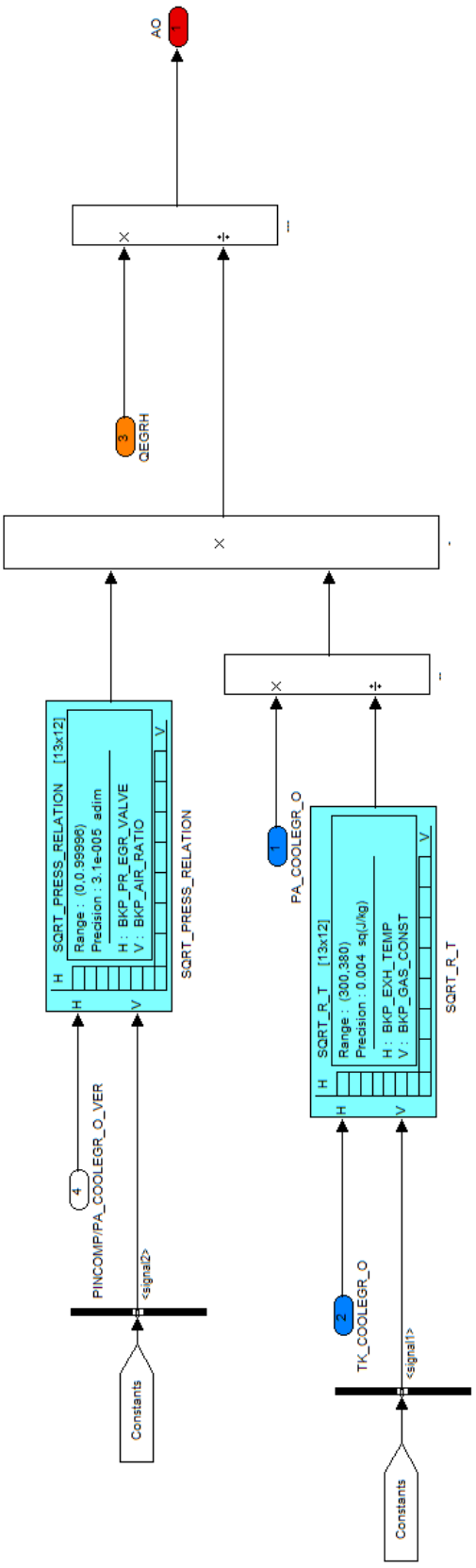

Figure 52: Internal view of Ao_Computation

MAP NAME	EQUATION
SQRT_PRESS_RELATION	$\sqrt{2\frac{k}{k-1}\left[\left(\frac{P_{out}}{P_{in}}\right)^{\frac{2}{k}} - \left(\frac{P_{out}}{P_{in}}\right)^{\frac{k+1}{k}}\right]}$
SQRT_R_T	$\sqrt{RT_{in}}$

Table 6: Table of the internal maps in Ao_Computation.

4.5.1 *SQRT_PRESS_RELATION map*

The first map corresponds to the first row in the Table 6, in this case the map was made using the equation that is shown and the available data. During the simulation process, the MDS program take the input data (PINCOM/PA_COOLEGR_O and k) and estimate the corresponding value.

The schematic representation for this map in Simulink format is shown in Figure (53).

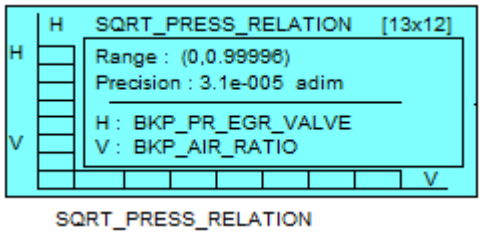

Figure 53: Schematic representation in Simulink format for SQRT_PRESS_RELATION map

4.5.2 *SQRT_R_T map*

In the second row of the Table 6 is shown the equation that was used for the second map corresponding to the square relation between the ideal gas constant and the inlet temperature for the EGR throttle valve (TK_COOLEGR_O). The respective graphical representation is shown in the Figure (54).

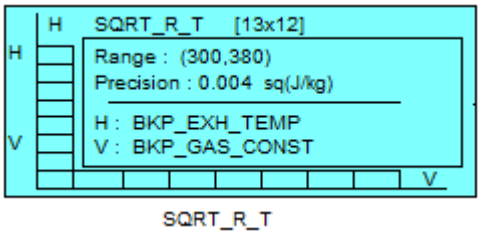

Figure 54: Schematic representation in Simulink format for SQRT_R_T map

The value for A_o is calculated by completing the rest of the equation with simple mathematical operations, as shown in Figure (52).

4.6 EGR_ANGLE

In the final step is performed the corresponding EGR_ANGLE, for this calculation are used the following entrances:

- AO value that was obtained in the previous section.
- Map for the create the relation between the EGR throttle valve angle and the A_o variable.

4.6.1 *AO_ANGLE_RELATION map*

The map was made using the same methodology that in the Sections 4.2.2 and 4.2.3 but considering the second database mentioned, where through a trendline is obtained the equation that gives the relation between the two parameters (Ao and the throttle valve angle). The equation in this case was:

$$EGR_{ANGLE} = -5,5E^{+17}(A_o)^4 + 2,0E^{+14}(A_o)^3 \\ -2,7E^{+10}(A_o)^2 + 1,6E^{+06}(A_o) - 2,8E^{+00} \quad (10)$$

As shown is a polynomial equation (Eq. 10) of order four, the selection procedure for the trendline consisted in choose the type of line that would give the highest possible accuracy. To find which of the different trendlines options available in Excel would be the most appropriate, the procedure below is followed:

1. Plotting of various types of trendlines for the same data, as shown the Figure (55).

2. Show the respective equation for each trendline (Table 7).

3. Calculate with the available data the EGR throttle valve angle using each equation.

4. Estimate which is the deviation between the real EGR throttle valve angle and the calculated for each case.

5. Perform the absolute summation of all the data and which is the average deviation from the real data.

6. Observe with which equation is obtained the lowest deviation value.

The results for the trendlines and the equations are represented in the Table 7 and Table 8.

For all the above, was deduced that the trendline with higher precision was the polynomial equation of order four, as can be seen in Table 8 due to has the lower deviation (3.69°) respect to the real EGR throttle valve angle.

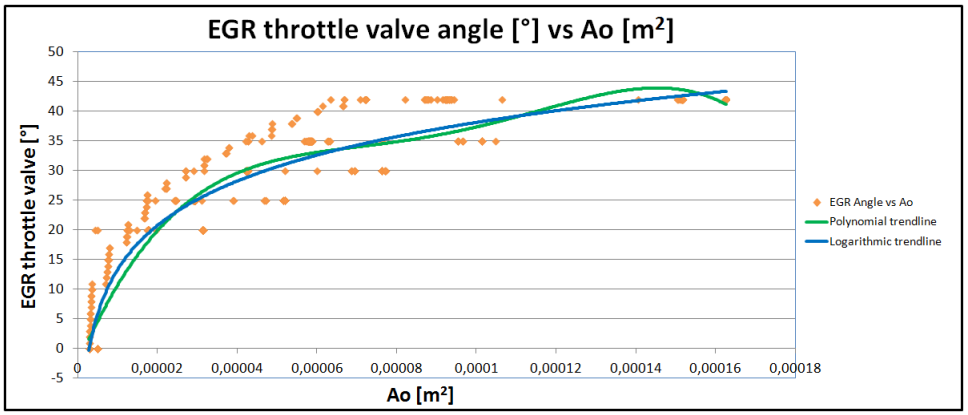

Figure 55: Ao vs EGR_ANGLE with the different trendlines

TRENDLINE	EQUATION
Polynomial	$EGR_{ANGLE} = -5,5E^{+17}(A_o)^4 + 2,0E^{+14}(A_o)^3$ $-2,7E^{+10}(A_o)^2 + 1,6E^{+06}(A_o)$ $-2,8E^{+00}$
Logarithmic	$EGR_{ANGLE} = 1,1E^{+01}ln(x) + 1,4E^{+02}$

Table 7: Trendline and corresponding equation.

TRENDLINE	DEVIATION [°]
Polynomial	3.692984
Logarithmic	4.637885

Table 8: Trendlines and the corresponding deviation.

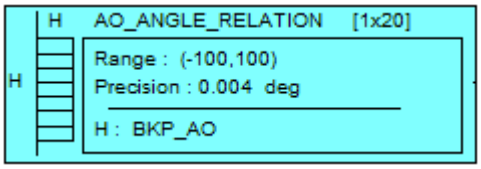

Figure 56: Schematic representation in Simulink format for AO_ANGLE_RELATION map

4.7 BOUNDARIES TO THE EGR THROTTLE VALVE ANGLE

After getting the angle, it passes through two filters that limit with a maximum and a minimum value. The limit values are the corresponding to the fully closed and fully open the valve. For the model, was established that the values are the following:

- Valve fully open: 52 °: the maximum was established considering the data from the engine, that for the maximum EGR mass flow was observed this value.
- Valve closed: 8°: the minimum angle was established take into account to prevent binding in the throttle bore, the throttle plate is usually completely closed at some nonzero angles.

In the Figure (57) is shown in details this part of the model.

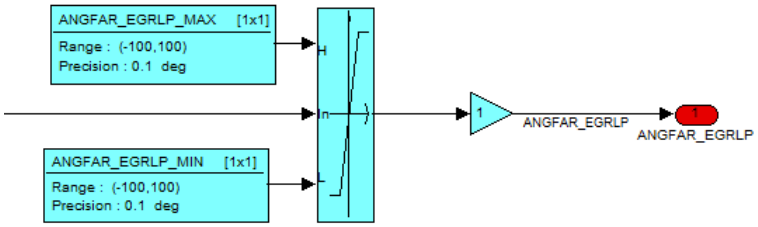

Figure 57: Boundaries to the EGR throttle valve angle

4.8 MODEL VERIFICATION PHASE

Now, the new model will be tested with a different data set to perform it, ie the rest of the database. The experiments were at:

1. 2500 rpm and 1500 mbar
2. 2500 rpm and 1500 mbar - Second Test
3. 2500 rpm and 1900 mbar
4. 4000 rpm and 1500 mbar

Already obtained the results of the simulation can be performed the comparison with the other two alternatives to solve the problem, which were described in Chapter 3, and see which option also allows more precise result to reality. It is important to point out that the Open Loop Map is not calibrated correctly due to missing data to build up the maps, so shown big difference angle values than other methods.

Below, is shown the common legend concerning the graphics where is compared the new model with the existents.

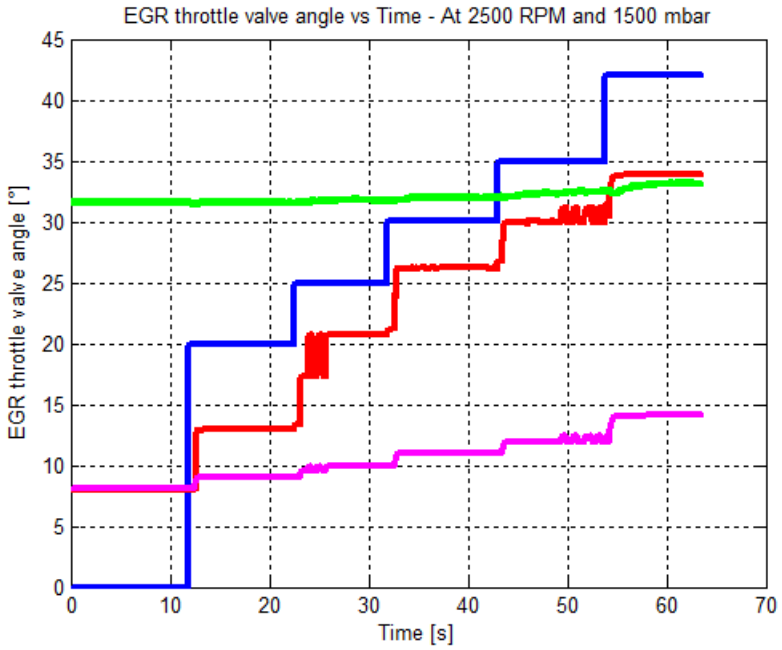

(a) 2500 rpm - 1500 mbar - The three models

Figure 58: Comparison between the three methods to obtain EGR throttle valve angle vs Time at 2500 rpm and 1500 mbar .

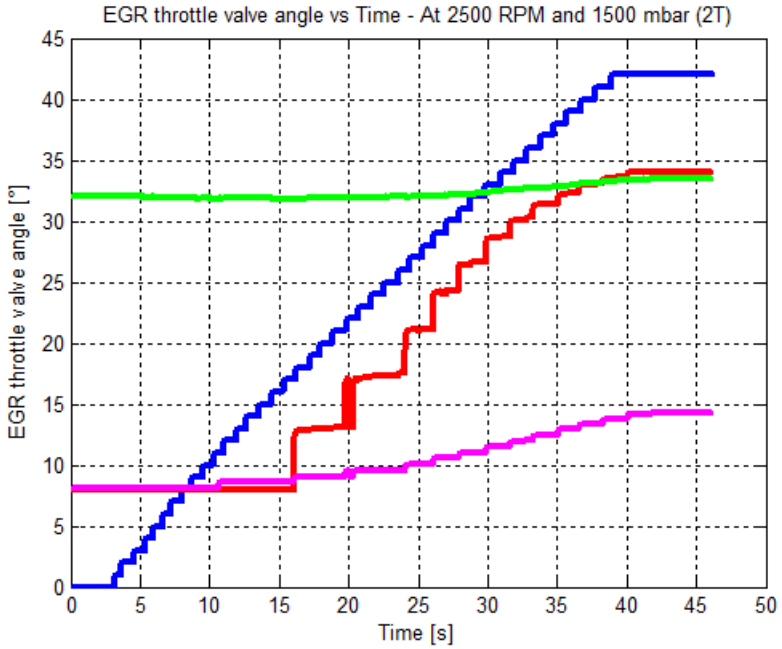

(a) 2500 rpm - 1500 mbar (2T) - The three models

Figure 59: Comparison between the three methods to obtain EGR throttle valve angle vs Time at 2500 rpm and 1500 mbar - Second test

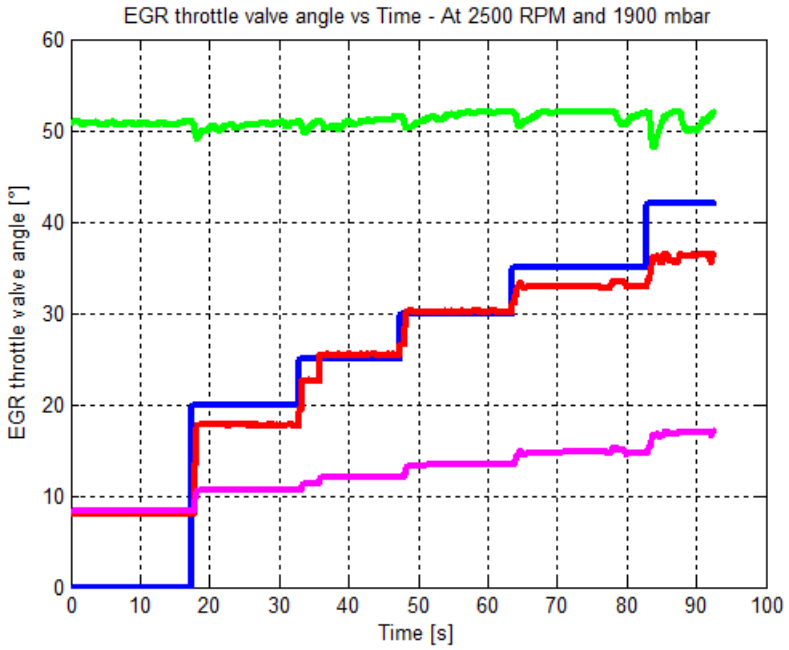

(a) 2500 rpm - 1900 mbar - The three models

Figure 60: Comparison between the three methods to obtain EGR throttle valve angle vs Time at 2500 rpm and 1900 mbar

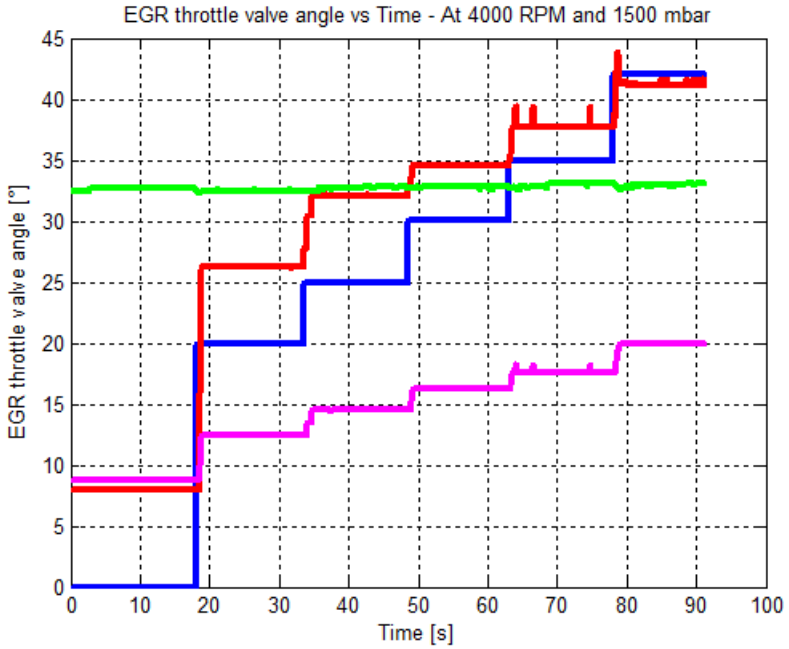

(a) 4000 rpm - 1500 mbar - The three models

Figure 61: Comparison between the three methods to obtain EGR throttle valve angle vs Time at 4000 rpm and 1500 mbar

As a general analysis of all graphics, highlights the fact that for the first three experiments carried out at 2500 rpm but different pressures (1500 and 1900 mbar), the curve obtained through the new model is below the actual result. Meanwhile, in the case of 4000 rpm and 1500 mbar, the curve is above.

At the same time, it can be seen that the result would be considered more reliable is the third experiment, the cause of this might be due to the formula applied, because this considered an example of all data obtained, wherein the third experiment would be within the limits that generate a reliable result.

Furthermore, other experiments could be considered the extremes of the database, generating a greater mistake.

One of the possible solutions that could be developed is to expand this database and in this way decrease the difference would generate.

In relation to the comparison with the other models in the different graphs shows that the new model produces a result with greater accuracy, which is an improvement to reach the goal of simulating the curve with high accuracy for any condition.

4.9 EGR THROTTLE VALVE ANGLE VS EGR MASS FLOW

The following section shows the four experiments that were used for the verification process, but this time it will plot the EGR throttle valve angle against the amount of EGR mass flow that should pass for each angle.

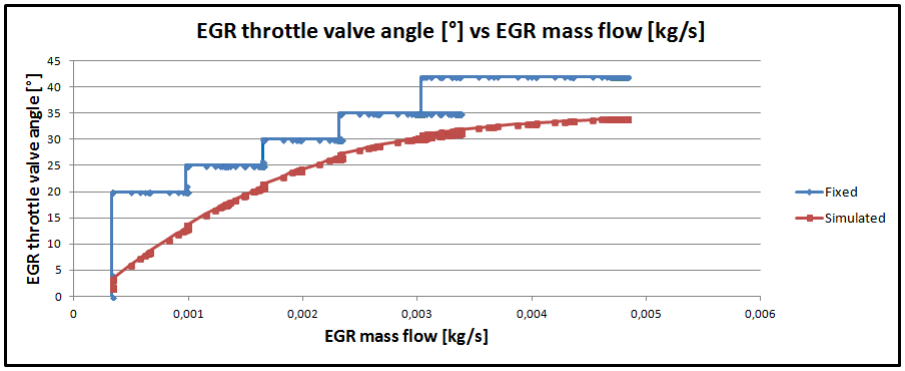

Figure 62: EGR throttle valve angle vs EGR mass flow - 2500 rpm and 1500 mbar

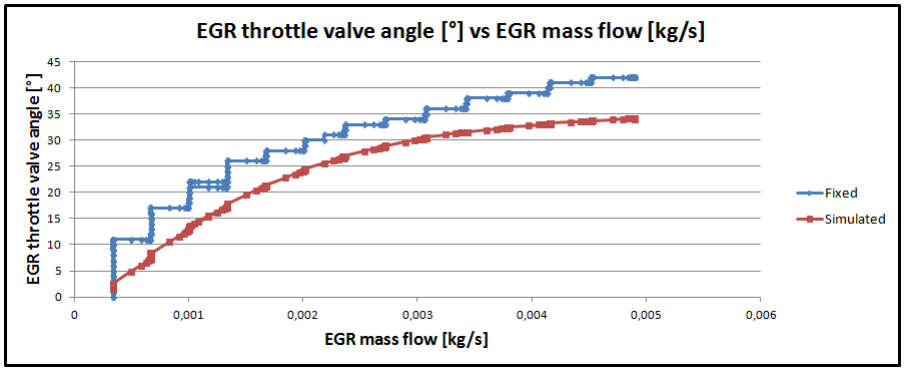

Figure 63: EGR throttle valve angle vs EGR mass flow - 2500 rpm and 1500 mbar (Second test)

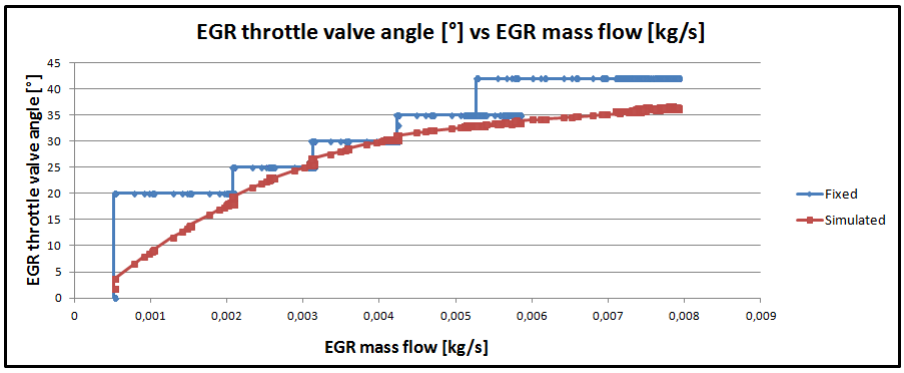

Figure 64: EGR throttle valve angle vs EGR mass flow - 2500 rpm and 1900 mbar

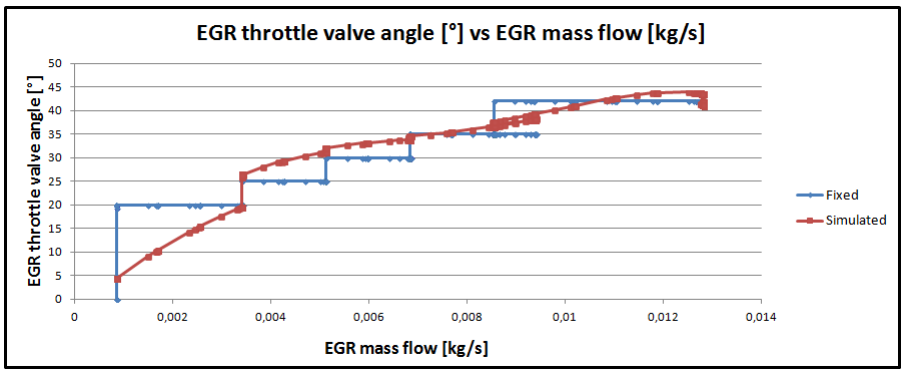

Figure 65: EGR throttle valve angle vs EGR mass flow - 4000 rpm and 1500 mbar

In the different graphs can be seen a similar behavior discussed in the previous section where the EGR throttle valve angle was plotted versus time.

The first two experiments it is observed that the data obtained through the simulator are below the fixed EGR throttle valve angle during each experiment, i.e. taking into account that was used as the fixed mass flow as reference and not simulated it; in the different curves the simulation results never reaches the expected EGR throttle valve angle (blue line).

For the third case, there is a small difference between the two results, fixed and simulated, which was also observed previously.

And finally to the case of 4000 rpm and 1500 mbar, there is a trend where the EGR throttle valve angle simulated is over the fixed in the experiment, but this difference is less than when compared against time.

4.10 COMPARISON BETWEEN THE FIXED AND SIMULATED

4.10.1 *For the EGR mass flow*

Now going to analyze the values of EGR throttle valve angle and the EGR mass flow separately, in other words, is compared in the same graph the fixed EGR throttle valve angle values and simulated against bisectrix, to see which is the deviation obtained through the model.

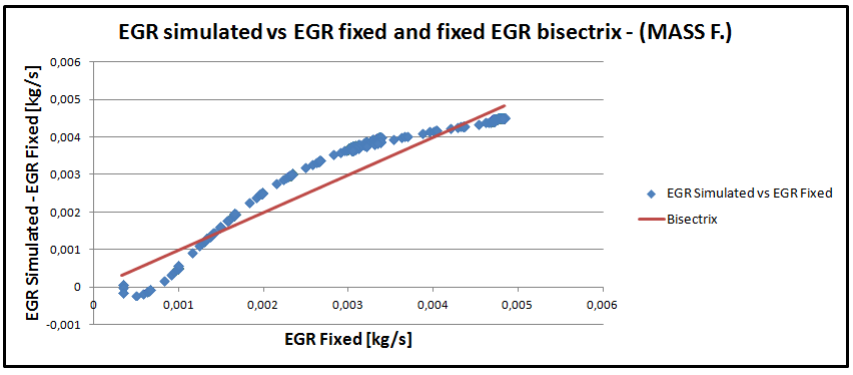

Figure 66: EGR calculated vs EGR fixed and fixed EGR bisectrix for the mass flow - 2500 rpm and 1500 mbar

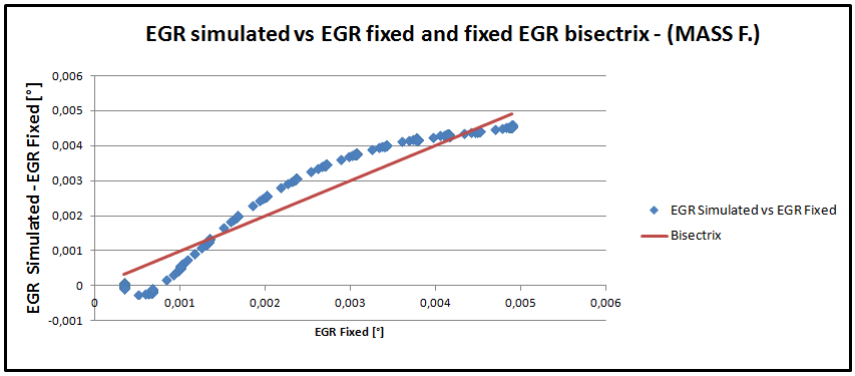

Figure 67: EGR calculated vs EGR fixed and fixed EGR bisectrix for the throttle valve angle - 2500 rpm and 1500 mbar

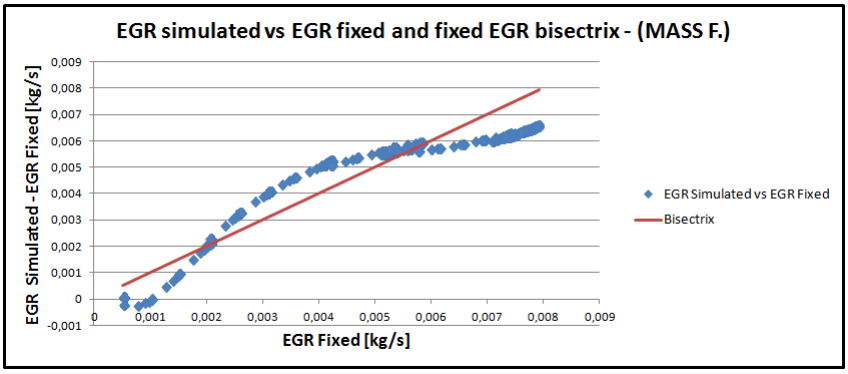

Figure 68: EGR calculated vs EGR fixed and fixed EGR bisectrix for the mass flow - 2500 rpm and 1500 mbar (Second test)

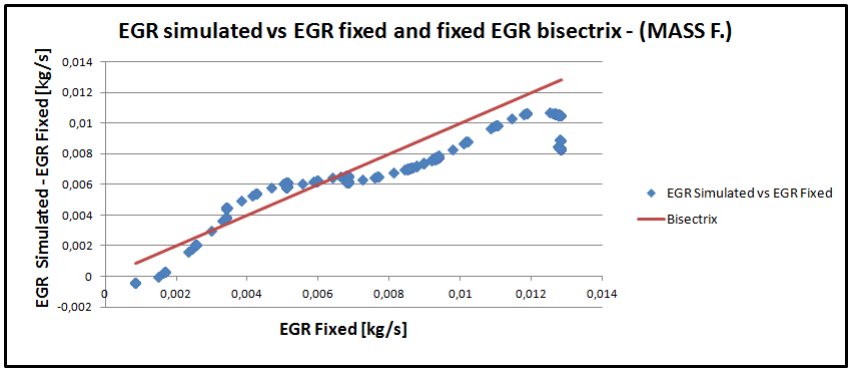

Figure 69: EGR calculated vs EGR fixed and fixed EGR bisectrix for the throttle valve angle - 2500 rpm and 1500 mbar

4.10.2 *For the EGR throttle valve angle*

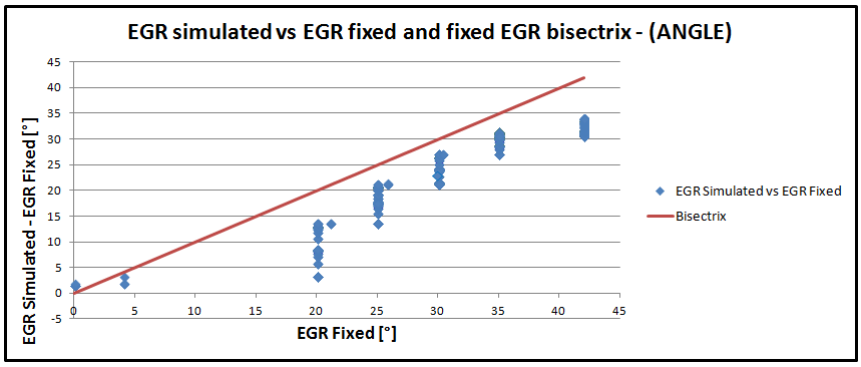

Figure 70: EGR calculated vs EGR fixed and fixed EGR bisectrix for the mass flow - 2500 rpm and 1900 mbar

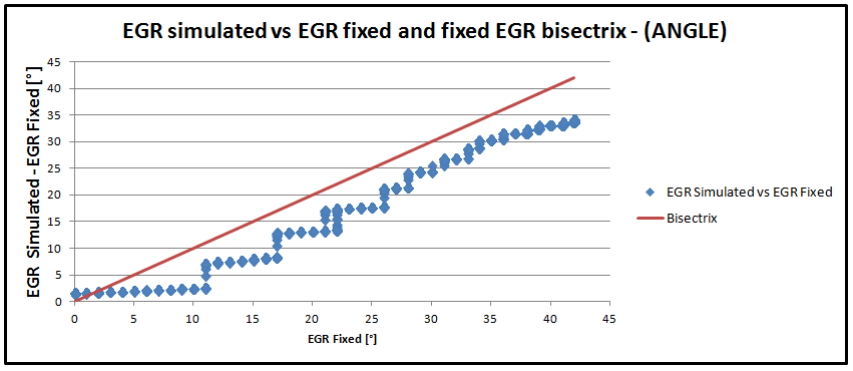

Figure 71: EGR calculated vs EGR fixed and fixed EGR bisectrix for the throttle valve angle - 2500 rpm and 1900 mbar

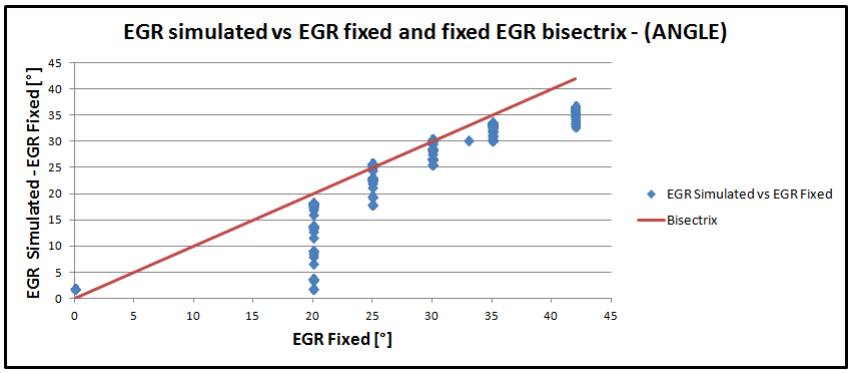

Figure 72: EGR calculated vs EGR fixed and fixed EGR bisectrix for the mass flow - 4000 rpm and 1500 mbar

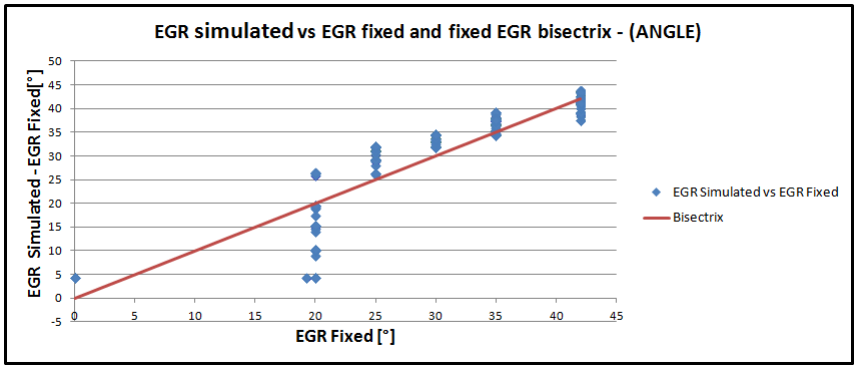

Figure 73: EGR calculated vs EGR fixed and fixed EGR bisectrix for the throttle valve angle - 4000 rpm and 1500 mbar

4.11 ABSOLUTE AND RELATIVE ERROR OF THE NEW EGR VALVE MODEL

After doing all the calculations and graphs, it is possible to represent absolute and relative errors for each experiment. Is noteworthy that the graphics were performed to compare the errors both in the case of the EGR throttle valve angle as to the EGR mass flow.

The following eight graphs are the absolute and relative errors with respect to the EGR throttle valve angle:

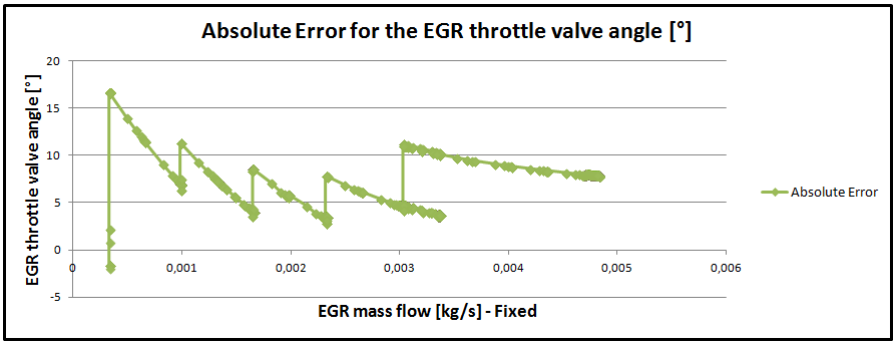

Figure 74: Absolute error for the EGR throttle valve angle with respect to the fixed data of the EGR mass flow - 2500 rpm and 1500 mbar

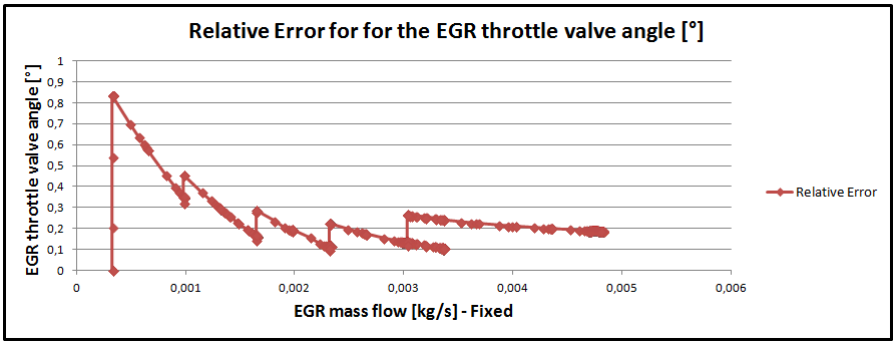

Figure 75: Relative error for the EGR throttle valve angle with respect to the fixed data of the EGR mass flow - 2500 rpm and 1500 mbar

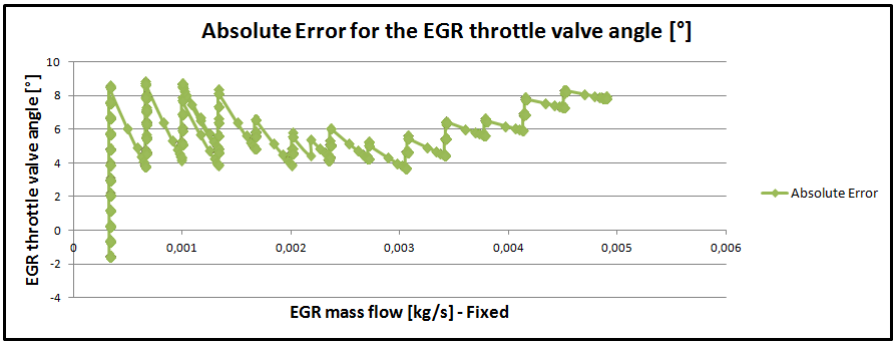

Figure 76: Absolute error for the EGR throttle valve angle with respect to the fixed data of the EGR mass flow - 2500 rpm and 1500 mbar (Second test)

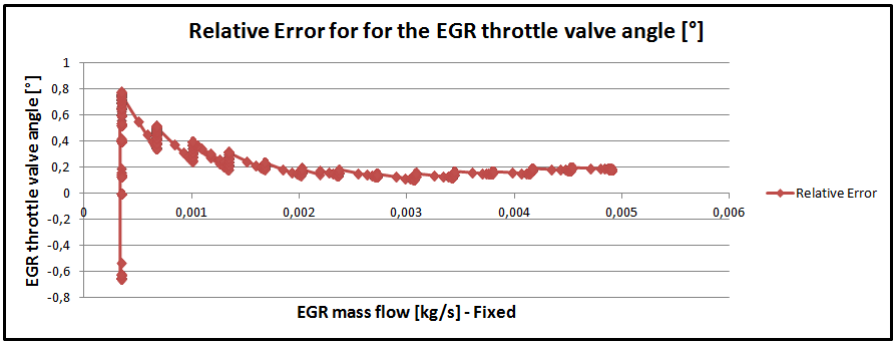

Figure 77: Relative error for the EGR throttle valve angle with respect to the fixed data of the EGR mass flow - 2500 rpm and 1500 mbar (Second test)

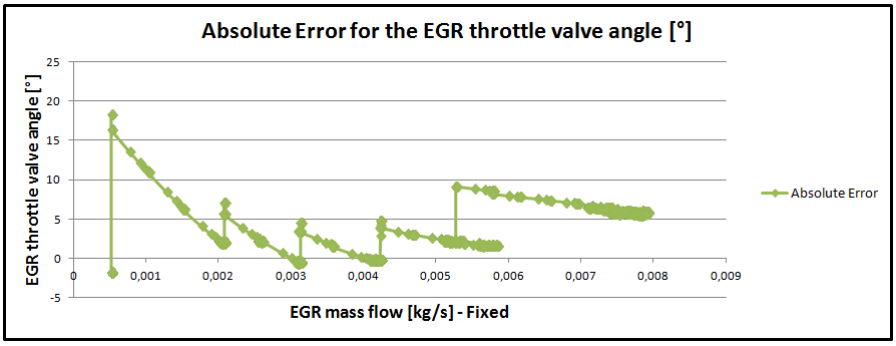

Figure 78: Absolute error for the EGR throttle valve angle with respect to the fixed data of the EGR mass flow - 2500 rpm and 1900 mbar

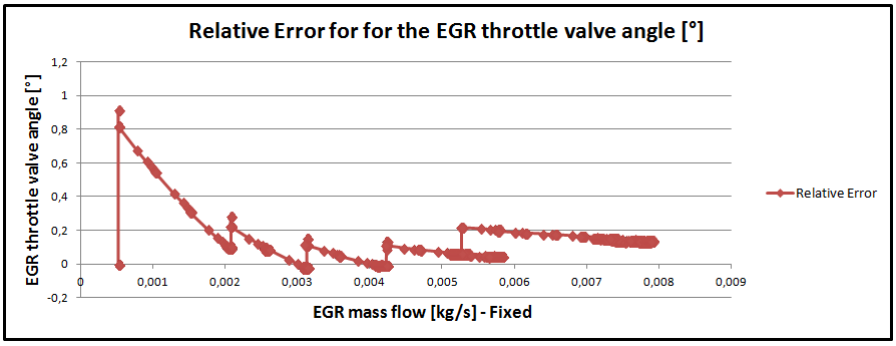

Figure 79: Relative error for the EGR throttle valve angle with respect to the fixed data of the EGR mass flow - 2500 rpm and 1900 mbar

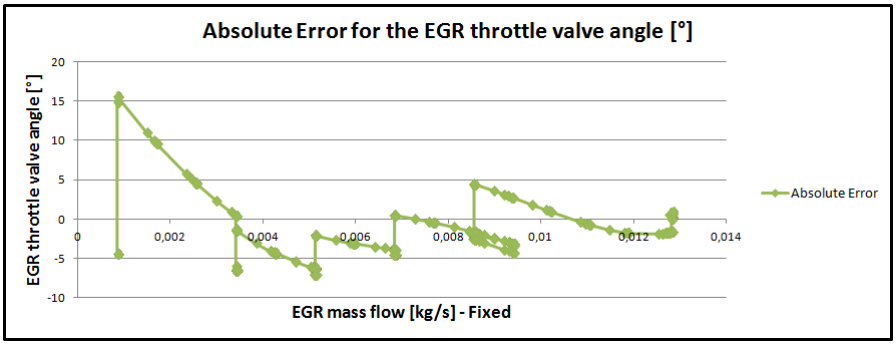

Figure 80: Absolute error for the EGR throttle valve angle with respect to the fixed data of the EGR mass flow - 4000 rpm and 1500 mbar

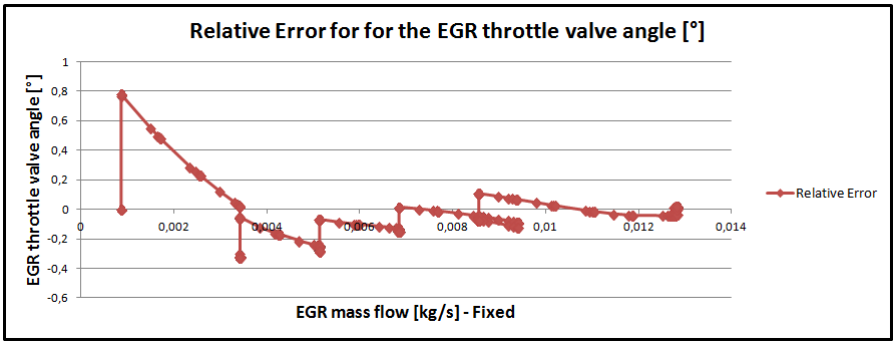

Figure 81: Relative error for the EGR throttle valve angle with respect to the fixed data of the EGR mass flow - 4000 rpm and 1500 mbar

For its part, the next eight are in relation to the EGR mass flow.

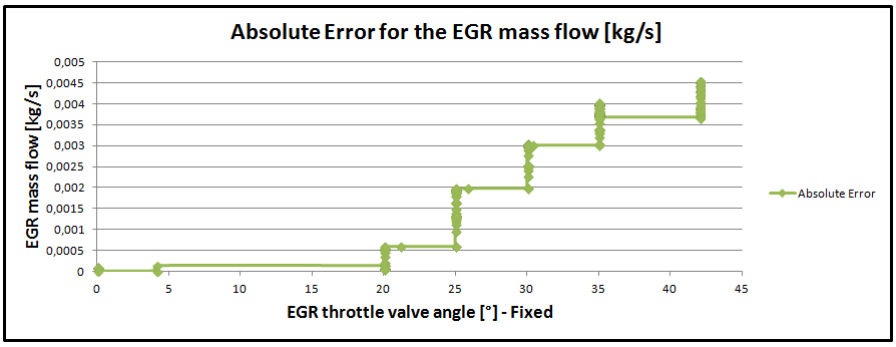

Figure 82: Absolute error for the EGR mass flow with respect to the fixed data of the EGR throttle valve angle - 2500 rpm and 1500 mbar

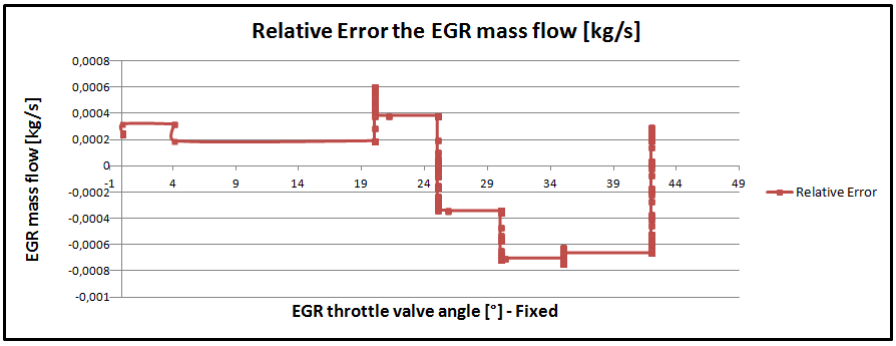

Figure 83: Relative error for the EGR mass flow with respect to the fixed data of the EGR throttle valve angle - 2500 rpm and 1500 mbar

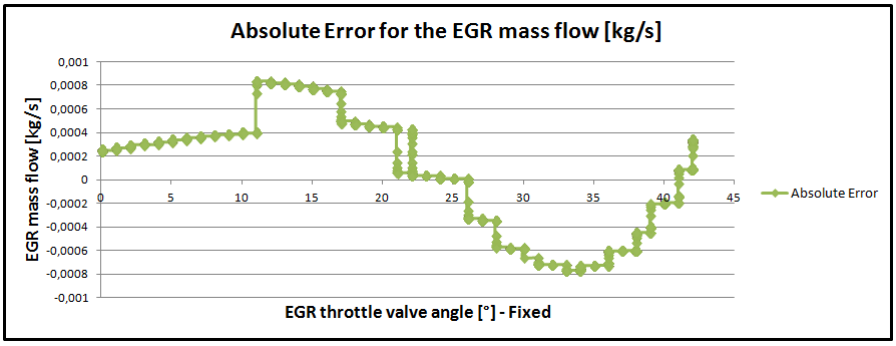

Figure 84: Absolute error for the EGR mass flow with respect to the fixed data of the EGR throttle valve angle - 2500 rpm and 1500 mbar (Second test)

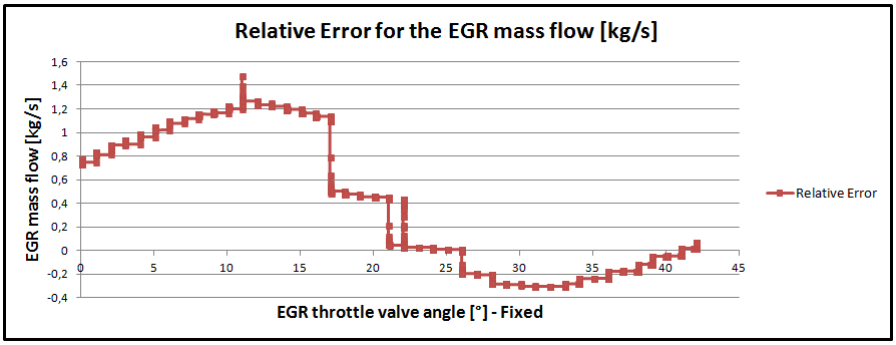

Figure 85: Relative error for the EGR mass flow with respect to the fixed data of the EGR throttle valve angle - 2500 rpm and 1500 mbar (Second test)

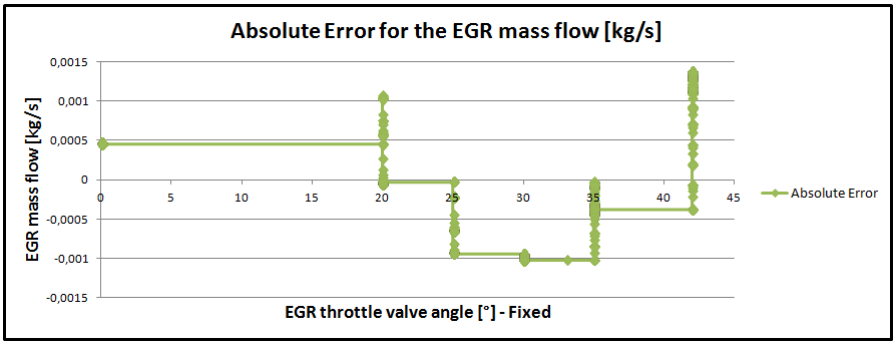

Figure 86: Absolute error for the EGR mass flow with respect to the fixed data of the EGR throttle valve angle - 2500 rpm and 1900 mbar

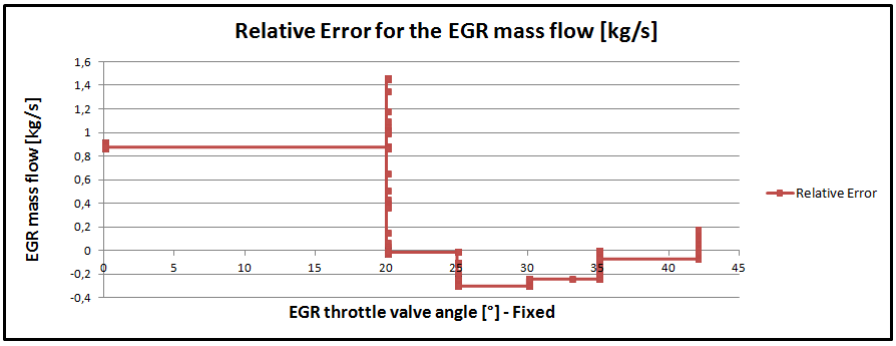

Figure 87: Relative error for the EGR mass flow with respect to the fixed data of the EGR throttle valve angle - 2500 rpm and 1900 mbar

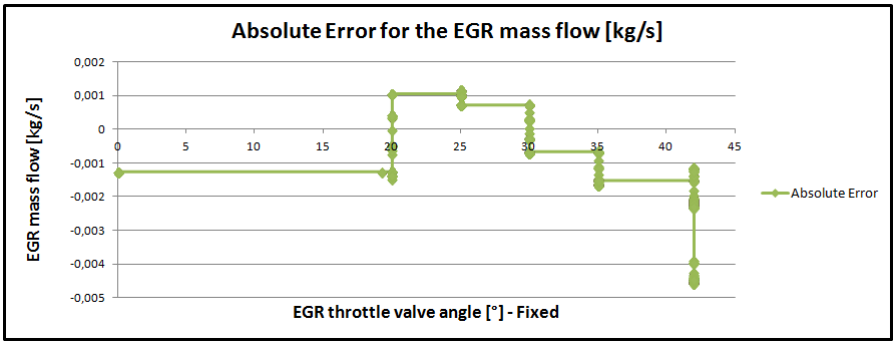

Figure 88: Absolute error for the EGR mass flow with respect to the fixed data of the EGR throttle valve angle - 4000 rpm and 1500 mbar

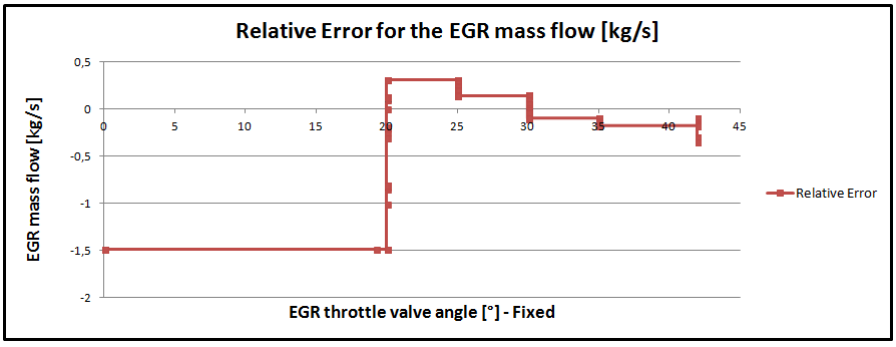

Figure 89: Relative error for the EGR mass flow with respect to the fixed data of the EGR throttle valve angle - 4000 rpm and 1500 mbar

5

CONCLUSION

The purpose of this work was developed a model to simulated the behaviour of EGR throttle valve in a Low Pressure EGR system. The model was performed in collaboration with the Centro Ricerche Fiat (C.R.F.).

The process of model construction was started analyzing the problem, existing solutions and studying the theoretical basis for propose a new possible solution.

Once collected all this information, and thanks to the database provided by Fiat was successfully developed the model. This new proposal is based on the theory of Compressible-Flow Nozzle equation in a flow that don't achieve the choked velocity, which later was reproduced in the Simulink and MDS software.

The new model consists firstly of a section where the data available in an engine (serial production) are converted in the needed to perform the calculation, since some of these data are not measured directly and are obtained through maps, specifically the case of the pressures and temperatures from outlet of the intercooler.

After, is the unit conversion section which takes each input parameter and converts the units required to perform the calculation. Also, there are two blocks that allow to avoid any error in the calculation, especially in the relation of the pressures.

Based on Compressible-Flow Nozzle equation, it was possible to obtain a parameter to be related to the EGR throttle valve angle that was called A_o, thanks to the data provided was obtained a trendline and the equation that allowed this relationship. Is important to note that were tested with two trendlines (logarithmic and polynomial) resulting polynomial as more accurate, therefore, was selected for use in the model.

The last phase for the construction of the model was to establish maximum and minimum limits for the EGR throttle valve angle, which in this case were 8 and 52 degrees respectively.

At the same time was held the verification phase for each of the 4 experiments (2500 rpm - 1500 mbar, 2500 rpm - 1500 mbar second test, 2500 rpm - 1900 mbar and 4000 rpm - 1500 mbar), obtaining as most precise the third experiment, which shows little difference between the EGR throttle valve angle set at the test bench and the simulated.

Simultaneously were plotted the EGR throttle valve angle against the EGR mass flow and the absolute and relative errors in each case.

As was found still remains a difference between the real behavior of the valve and the simulation performed, for this reason, below are disclosed some points where it is possible improve or change the model thus achieve most accurate results.

- Improvement of the data acquisition process to build maps so that yield a more accurate result, ie, establish clear conditions in which the valve will be evaluated, expand the ranges in which data are collected (more rpm) and finally attempt to establish a single experiment to evaluate the valve to avoid further discrepancies.

- Add the appropriate delay so take into consideration this parameter too, ie a more realistic result.

Part III

APPENDIX

A

COMMONLY USED SYMBOLS AND ABBREVIATIONS

A.1 SYMBOLS

Table 9: Symbols and the description.

SYMBOLS	DEFINITION
a	Relation between shaft diameter and throttle bore diameter
ANGFAR_EGRLP	Throttle valve angle for exhaust gas recirculation low pressure system
A_o	Parameter that contain the discharge coefficient and the throttle plate open area
A_{th}	Open area
C_D	Discharge coefficient
d	Shaft diameter
CEGR_Main_Calc	There is the ability to chose the model to evaluate the target EGR throttle plate position with the delay and closed loop PI
CEGR_Setup_Call	Section in which all the values are resets and is established as default zero to start
CEGR_Scheduler	Representation of the different available events in the CEGR model
CQLC	Model that provide the Exhaust gas recirculation intake capacity

SYMBOLS	DEFINITION
D	Throttle bore diameter
EGR_ANGLE	Throttle angle for low pressure exhaust gas recirculation
ETAEGRMAX	Maximum normalized estimated external EGR mass that the engine can aspirate
ETASPOBJ	Target intake efficiency
ev_PowerOn	Event when the switch is passed without strat the cranking phase
ev_MediumTime	Event that occur every 12 ms, the different sensors are reglated each interval time
IASP	Model that provide the air intake capacity
k	Heat capacity ratio
°K	Kelvin
$\dot{m}_{EGR}$	Mass flow rate of EGR
$\dot{m}_{th}$	Mass flow rate across the throttle plate
PA_COOLEGR_O	Vector for the output absolute pressure of the exhaust gas recirculation intercooler
PCAT_PINT_RELATION	Map for the catalyst and exhaust gas recirculation intercooler pressure relation
PEXHO2SENS	Output pressure of the catalyst
PINCOMP	Input compressor pressure
PINCOMP/PA COOLER_O	Pressure relation
PINCOMP/PA COOLER_O_VER	Pressure relation verified
$P_{in} = p_0$	Upstream pressure of the throttle plate, input pressure of the convergent nozzle

SYMBOLS	DEFINITION
$P_{out} = p_T$	Downstream pressure of the throttle plate, output pressure of the convergent nozzle
QAH	Air intake capacity per hour for all cylinders
QEGRH	Exhaust gas recirculation intake capacity per hour for all cylinders
QEGRH_MAX	Maximum quantity of exhaust gas recirculation intake capacity per hour for all cylinders
QEGRH_MIN	Minimum quantity of exhaust gas recirculation intake capacity per hour for all cylinders
R	Generical radical, ideal constant gas
SQRT_PRESS_RELATION	Map for the square pressure relation
SQRT_R_T	Map for the square temperature and ideal gas constant relation
TB_LPEGR_INVMDL_ANG	Table low pressure exhaust gas reciruclation inverse model angle
$T_{in} = T_0$	Upstream temperature of the throttle plate, input temperature of the convergent nozzle

A.2 ABBREVIATIONS

PARAMETER	DEFINITION
(A/F)	Air fuel ratio
BC	Bottom center
DPF	Diesel Particulate Filter
ECU	Engine control unit
EGR	Exhaust gas recirculation
EIVC	Early intake valve closing
FL	Full lift
GDI	Gasoline direct injection
HP	High pressure
LIVO	Late intake valve opening
INCA	Integrated calibration and acquisition system
LP	Low pressure
MAF	Mass air flow
MATLAB	Matrix laboratory
MBT	Maximum brake-torque
MDS	Model development strategies
MEP	Mean effective pressure
ML	Multi lift
PFI	Port fuel injection
PM	Particle matter
RPM	Revolution per minute
SI	Spar ignition
TC	Top center
TDC	Top dead center
TWC	Three ways catalyst
VGT	Variable feometry turbocharger
WOT	Wide open throttle

Table 10: Abbreviations.

BIBLIOGRAPHY

[1] John B. Heywood. *Internal Combustion Engine Fundamentals*. McGraw-Hill, New York, USA, 1989.

[2] Federico Millo. *Engine Emissions Control*. Course notes, Politecnico di Torino, Italia, 2013.

[3] E. Galloni G. Fontana. "Experimental analysis of a spark-ignition engine using exhaust gas recycle at WOT operation". *ELSEVIER*, vol. 87: pp. 2187–2193, June 2010. [Online]. Available: http://www.journals.elsevier.com/applied-energy.

[4] G. Alla. "Using exhaust gas recirculation in internal combustion engines: A review". *ELSEVIER*, vol. 43: pp. 1027–1042, April 2001. [Online]. Available: http://www.journals.elsevier.com/energy-conversion-and-management.

[5] S. Sinha M. Shukla A. Agrawal, S. Singh. "Effect of EGR on the exhaust gas temperature and exhaust opacity in compression ignition engines". *Sadhana*, vol. 29: pp. 275–284, June 2004. [Online]. Available: http://www.ias.ac.in/sadhana/Pdf2004Jun/Pe1131.pdf.

[6] P. Anderssoni A. Banks, M. Niven. "Boosting technology for Euro vi and tier 4 final heavy duty diesel engines without NOx aftertreatment". *Ricardo Consulting Engineers Ltd*, vol. 1: pp. 35–47, 2010. [Online]. Available: http://www.imeche.org/docs/default-source/turbocharging-papers/4_Boosting_technology_for_euro_VI_and_tier_4_final_heavy_duty_diesel_engines_without_NOx_aftertreatment.pdf?sfvrsn=0.

[7] J. Suryavanshi P. Ghodke. "Review of advanced EGR and Breathing Systems for High Performance and Low Emission HSDI Diesel Engine". *International Journal of Modern Engineering Research (IJMER)*, vol. 2: pp. 3138–3142, October 2012. [Online]. Available: http://www.ijmer.com/papers/Vol2_Issue5/AF2531383142.pdf.

[8] B. Pla W. Linares V. Bermudez, J. Lujan. "Effects of low pressure exhaust gas recirculation on regulated and unregulated gaseous emissions during NEDC in a light-duty diesel engine". *ELSEVIER*, vol. 36: pp. 5655–5665, July 2011. [Online]. Available: http://www.journals.elsevier.com/energy.

[9] F. Borean F. Gustinetti, G. Cinicola. RASP and IASP Modules. *Fiat PowerTrain*, 2009.

[10] G. Shu L. Tan Y. Wang H. Wei, T. Zhu. "Gasoline engine exhaust gas recirculation - A review". *ELSEVIER*, vol. 99: pp. 534–544, June 2012. [Online]. Available: http://www.journals.elsevier.com/applied-energy.

[11] Z. Dimitrova T. Alger, T. Chauvet. "Synergies between High EGR Operation and GDI Systems". *SAE Int. J. Engines*, vol. 1: pp. 101–114, April 2001.

[12] Lorenza Magnani. *Manuale Matlab Simulink e Control System*. AIAP, Pavia, Italia, 2005.

[13] F. Gustinetti. Modelization Development Strategies (MDS). *Centro Rierche Fiat*, Version 9.0, Torino, Italia.

[14] MathWorks. Documentation Center. [Online]. Available: http://www.mathworks.com.

[15] Gasiorek J. M. Swaffield J. A. Douglas, J. F. and B. L. Jack. *Fluid Mechanics*. Pearson, Ammanford, A., United Kingdom, 2008.

[16] G. A. Goodenough. *Principles of Thermodynamics*. Henry Holt and Company, New York, USA, 1931.

[17] Okcc "Precision Orifice Capital of the World". O'keefe Controls Co. [Online]. Available: http://www.okcc.com/PDF/Choked

[18] E. Spessa S. d'Ambrosio, A. Ferrari. "Analysis of the egr system performance in modern diesel engines". *Journal of Engineering for Gas Turbine and Power*, vol. 135 / 081601, August 2013.

[19] Claudio Martucci. *"Caratterizzazione modelo automotive per un sistema hardware in the loop"*. Master Thesis, Torino, Italia. Politecnico di Torino. (2012).

[20] R. Palmaccio E. Galloni, G. Fontana. "Effects of exhaust gas recycle in a downsized gasoline engine". *ELSEVIER*, vol. 105: pp. 99–107, January 2012. [Online]. Available: http://www.journals.elsevier.com/applied-energy.

[21] Frank M. White. *Fuid Mechanics*. McGraw-Hill, New York, USA, 4th edition, 2002.